

HYDROXYAPATITE COATING ON 316L STAINLESS STEEL BY DIP COATING
METHOD

by

Sezen Dedeođlu

B.S, Mechanical Engineering, Yıldız Technical University, 2007

Submitted to the Institute for Graduate Studies in
Science and Engineering in partial fullfilment of
the requirements for the degree of
Master of Science

Graduate Program in Mechanical Engineering

Bogazici University

2013

ACKNOWLEDGEMENTS

I would like to express my gratitude to my advisor, Prof. Sabri Altıntaş for the opportunity to work in this project. I was very fortunate to have his passion, guidance, and constant support throughout my graduate years. Additionally, I would like to acknowledge Assist. Prof. Mehmet İpekođlu and Nazım Mahmutyazıcıođlu for their valuable advice and suggestions.

I would like to thank my mother Nevin Kavak, and my brother Volkan Dedeođlu for their unwavering encouragement and support during my education at Bođazici University. I am appreciative of my parents for their wise and patient advice.

I would like to express my sincere appreciation to all my colleagues for their help and friendship. In particular, Mehmet İpekođlu for his contributions as my supervisor in this project. I also wish to thank Bilge Gedik Uluocak at the Bođazici University Advanced Technologies Center for her help with scanning electron microscopy and EDS analysis.

This work was supported by The Scientific & Technological Research Council of Turkey (TUBİTAK) through the project 107M556. I would like to thank TUBİTAK for financially supporting me as a graduate student throughout the project.

ABSTRACT

HYDROXYAPATITE COATING ON 316L STAINLESS STEEL BY DIP COATING METHOD

Hydroxyapatite (HA) coating on 316L Stainless steel with different amounts of polyvinyl alcohol (PVA) additive and different sintering temperatures were fabricated by using dip coating method. Hydroxyapatite was inoculated with polyvinyl alcohol which was used as surfactant and binder in the composition to obtain adherent, uniform and crack free coatings. The compositions of PVA to deionized water in the mixture are 5 %, 7.5 % and 10 % wt. and the HA amount in the compositions are kept stable at 15 %. The films were subjected to heat treatment at temperatures 500 °C, 700 °C and 800 °C in an atmospheric oven. In the second step, the coated samples were subjected to heat treatment at 800 °C, 900 °C and 1000 °C under vacuum to increase the bonding between the substrate and the HA and to enhance corrosion resistance. The composition of hydroxyapatite slurry and the sintering temperature both affected the morphology of the coatings. Stereo microscope and scanning electron microscopy (SEM) were used to characterize the surface morphology of the coatings. The open porosity and pore connectivity were enhanced with PVA additive in the vacuum furnace. Also, it was observed that at 1000 °C sintering temperature, films start to peel off from the substrate due to the mismatch of the thermal expansion coefficient of the metal substrates and the HA.

ÖZET

DALDIRMA KAPLAMA METODUYLA 316L PASLANMAZ ÇELİK ÜZERİNE HİDROKSİAPATİT KAPLANMASI

Farklı sıcaklık değerlerinde ve farklı polivinil alkol (PVA) miktarlarında 316L paslanmaz çelik üzerine hidroksiapatit (HA) kaplanması daldırma kaplama yöntemiyle gerçekleştirilmiştir. Homojen, bağlanmış ve çatlaksız bir kaplama elde etmek için HA, yüzey etkinleştirici ve bağlayıcı madde olarak kullanılan PVA ile karıştırılmıştır. Bu bileşimde HA ağırlık oranı 15 % olarak sabit tutulurken, PVA'nın iyonsuz suya ağırlık olarak oranı sırasıyla 5 %, 7.5 % ve 10 % olarak alınmıştır. Elde edilen filmler atmosferik fırında 500 °C, 700 °C and 800 °C de ısı işleme maruz bırakılmıştır. İkinci süreçte, altlıklar ile hidroksiapatitin birbirine daha iyi bağlanması ve korozyon dayanımını arttırmak amacıyla kaplanan numuneler 800 °C, 900 °C and 1000 °C vakum fırınında ısı işleme tabi tutulmuştur. Hem HA karışım oranları hem de sinterleme sıcaklığının kaplamanın yüzey yapısını etkilediği görülmüştür. Kaplamaların yüzey yapısını gözlemek amacıyla stereo mikroskop ve tarama elektron mikroskobu (SEM) kullanılmıştır. Vakum fırında yapılan deney sonuçlarında açık gözenekler ve gözenekler arası iletim PVA eklenmesiyle elde edilmiştir. Ayrıca 1000 °C sinterleme sıcaklığında, metal altlık ile HA'nın farklı ısı genleşme katsayılarındaki uyumsuzluk sebebiyle, filmlerin yüzeyinde soyulmaların olduğu gözlemlenmiştir.

TABLE OF CONTENTS

ACKNOWLEDGEMENTS	iii
ABSTRACT	iv
ÖZET	v
LIST OF FIGURES	viii
LIST OF TABLES	xi
LIST OF SYMBOLS	xii
LIST OF ACRONYMS / ABBREVIATIONS	xiii
1. INTRODUCTION.....	1
2. SCIENTIFIC BACKGROUND	3
2.1. Biomaterials and Their Applications.....	3
2.1.1. Metallic Biomaterials.....	3
2.1.2. Ceramics	6
2.1.3. Polymers	7
2.1.4. Composite Materials	9
2.2. Calcium Phosphate Minerals.....	9
2.2.1. Calcium Phosphate Minerals	9
2.2.2. Hydroxyapatite	11
2.3. Hydroxyapatite Coating Techniques	14
2.3.1. Electrophoretic deposition	14
2.3.2. Thermal Spraying	14
2.3.3. Plasma Spray Coating.....	15
2.3.4. Biomimetic Method	16
2.3.5. Sol-gel Method	17
2.3.6. Dip Coating Method	18
3. MATERIALS AND METHODS	23
3.1. Materials Preparation	24
3.2. Dip Coating Solution Preparation	24
3.3. Deposition of Sol-Gel HA Thin Films	26

3.3.1. Heat Treatment	26
3.3.1.1. Sintering.	26
4. RESULTS AND DISCUSSIONS	30
4.1. The effect of Solution Ingredients on Coating	30
4.2. The Effect of Withdrawal Times and GEL concentrations	31
4.3. The Effect of PVA additive	33
4.4. The Effect of Sintering Temperature.....	36
4.4.1. Different Sintering Temperature in Air Furnace	36
4.4.2. The Effect of Sintering Temperature in Vacuum	41
4.5. Crack Ocurance	46
4.6. EDAX Results	47
5. CONCLUSIONS	48
REFERENCES	49

LIST OF FIGURES

Figure 2.1.	Typical stress–strain relationships of a variety of bone implants [19].	6
Figure 2.2.	The crystal structure of HA [31].	12
Figure 2.3.	Schematic representation of sol-gel method	17
Figure 3.1.	The equipment designed for dip coating method.....	23
Figure 3.2.	Process flowchart of the preparation of the HA dip-coating solution [10].....	25
Figure 3.3.	Schematic of the paths for surface energy reduction in sintering. a) coarsening where small particles combine to form larger-sized particles and 2 is b) the densification of particles followed by grain growth [53].	27
Figure 3.4.	Schematic representation of the neck formation during solid-sintering due to (a) powder compaction, (b) neck growth, and (c) neck growth accompanied by densification. [53]	28
Figure 4.1.	Camera images of samples(a) Set 1, (b) Set 2, (c) Set 3, (d) Set 4.....	30
Figure 4.2:	Stereo microscope images of samples (a) Set 1, (b) Set 2, (c) Set 3, (d) Set 4 ..	31
Figure 4.3.	Camera images of samples(a) Set 4, (b) Set 5, (c) Set 6, (d) Set 7.....	32
Figure 4.4.	Stereo microscope images of samples (a) Set 5, (b) Set 6, (c) Set 7, (d) Set 8...	33
Figure 4.5.	Digital camera images of samples (a) Set 9, (b) Set 10, (c) Set 11, (d) Set 12...	34
Figure 4.6.	Stereo microscope images (a) Set 9, (b) Set 10, (c) Set 11, (d) Set 12.....	35

Figure 4.7.	Digital camera image of the the sample in set 13	37
Figure 4.8.	Stereo microscope image of the samples (a) set 13, (b) set 14, (c) set 15	37
Figure 4.9.	EM images of the surface of the the sample in set 13	38
Figure 4.10.	Digital camera image of the sample in set 14.....	39
Figure 4.11.	SEM images of the surface of the sample in set 14.....	39
Figure 4.12.	Digital camera image of the sample in set 15.....	40
Figure 4.13.	SEM images of the surface of the sample in set 15	41
Figure 4.14.	Digital camera image of the sample in set 16.....	41
Figure 4.15.	Stereo microscope image of the samples (a) set16, (b) set17, (c) set 18.....	42
Figure 4.16.	SEM images of the surface of the sample in set 16.....	43
Figure 4.17.	Digital camera image of the sample in set 17.....	44
Figure 4.18.	SEM images of the surface of the sample in set 17	44
Figure 4.19.	Digital camera image of the sample in set 18.....	45
Figure 4.20.	SEM images of the surface of the sample in set 18.....	45
Figure 4.21.	Digital camera image of sample with cracks	46
Figure 4.22.	Stereo microcope images of a sample with cracks	46
Figure 4.23.	EDAX results of the sample in set 17.....	47

Figure 4.24. EDAX results of the sample in set 18..... 47

LIST OF TABLES

Table 2.1.	Mechanical properties of metallic biomaterials.	5
Table 2.2.	Mechanical properties of typical polymeric biomaterials.	8
Table 2.3.	Physical Properties of Calcium Phosphates.	10
Table 2.4.	The major calcium phosphates.	11
Table 2.5.	Physicochemical, mechanical, and biological properties of HA [33].	13
Table 2.6.	Some coating techniques and their advantages - disadvantages. [34]	21
Table 2.7.	Process parameters used in some studies about HA coating.	22
Table 4.1.	Different Amount of Ingredients for Solution Preparation	30
Table 4.2.	Effect of Withdrawal Times and GEL concentration	32
Table 4.3.	Effect of different PVA additive to the solutions.	34
Table 4.4.	Effect of Sintering Temperature in air furnace	37
Table 4.5.	Effect of Sintering Temperature in vacuum.	41

LIST OF SYMBOLS

h	Coating Thickness
U_o	Withdrawal rate
g	Gravitational acceleration
γ_{lv}	Liquid-vapor surface tension
η	Solution viscosity
ρ	Density

LIST OF ACRONYMS / ABBREVIATIONS

ACP	Amorphous calcium phosphate
Ca-P	Calcium phosphate
EDXA	Energy dispersive x-ray analysis
FDA	Food and Drug Administration
HA	Hydroxyapatite
HCA	Hydroxy carbonate apatite
IPA	Isopropyl alcohol
PGA	Polyglycolic acid
PLA	Polylactic acid
PVA	Polyvinyl alcohol
SEM	Scanning Electron Microscopy
TEM	Transmission Electron Microscopy
XRD	X-ray diffraction

1. INTRODUCTION

The term 'osseointegration' was first introduced by Branemark [1] to describe the contact between the surface of a load-bearing artificial implant and the bone. The requirements for stable interface and faster osseointegration between the tissues and the implant lead researchers to investigate materials which have both high capacity to interact and bond chemically with the surrounding tissues and also adequate mechanical strengths. Among the various biomaterials available, hydroxyapatite ($\text{Ca}_{10}(\text{PO}_4)_6(\text{OH})_2$) gains more importance than others due to its chemical similarity to natural bone and its excellent biocompatibility and bioactivity. However, the brittle nature of hydroxyapatite cannot meet the requirements that an implant has to have in load bearing zones. When it comes to metals like austenitic stainless steels, titanium and its alloys, cobalt-chromium alloys, 316L stainless steel which are used in implant purposes, 316L stainless steel has gained popularity owing to its high corrosion resistance, mechanical properties and low cost. Although, 316L stainless steel exhibits high strength and toughness in clinical applications for restoration of anatomical systems, it is susceptible to chemical degradation after long term uses. Clinical experiments have shown that it is susceptible to localized corrosion in the human body causing the release of metal ions into the tissues surrounding the implants [2, 3]. Therefore hydroxyapatite coating has been applied on metal substrates to sustain stable fixation between the bone and the implant while metal substrates act as load bearing units.

Many techniques have been investigated for the coating of hydroxyapatite on metallic substrates, including plasma spraying, ion beam sputtering, chemical vapour deposition, laser sputtering, electrophoresis, electrochemical deposition and dip coating [5-8]. Among these techniques most reported works have focused on the dip coating of hydroxyapatite coatings [9-12]. The reason for the interest in dip coating of hydroxyapatite on metal substrate arises from the possibility to obtain stoichiometric, high purity coatings on complex shaped materials, ease of obtaining the desired thickness and high layer adhesion to the substrate.

In this thesis, HA was used as a ceramic biomaterial because of it is similar composition with the natural bone, its bioactive and biocompatibility nature which allows to form bonding directly with living tissue; whereas its brittle and hard properties hinder us to use it alone. To prevent these detrimental effects of HA, it was coated on metal substrates.

Stainless steel was chosen as metallic biomaterials because of its high strength properties, biocompatibility nature and low cost advantage. The coatings were obtained by dip coating method since this coating method has advantages like coating complex shapes, inexpensive, obtaining uniform and homogenous coating at the end.

For dip coating of HA on stainless steel in order to understand crack occurrence reasons, find way to eliminate them and to investigate the effect of parameters, the surface morphology of HA coating on type 316L stainless steel a study involving changing gelatin and PVA additive ratio in the suspension, altering withdrawal times and sintering temperature was performed. In the next step by obtaining the crack free coatings, adjusting the sintering temperature under air atmospheres and under vacuum was performed and characterized.

2. SCIENTIFIC BACKGROUND

2.1. Biomaterials and Their Applications

A biomaterial can be defined as any substance or combination of substances which have synthetic or of natural origin, and can be used as a part of a system which treats, augments or replaces any tissue, organ, or a function of the body [17]. There are mainly four groups of solid biomaterials. These are metals, polymers, ceramics, and composites. Since the structures of these materials differ, they have different properties and, therefore, different uses in the body.

2.1.1. Metallic Biomaterials

Metallic biomaterials are used as biomaterials due to their excellent electrical and thermal conductivity, mechanical properties (high tensile and fatigue strength) and biocompatibility [18]. They have been used predominantly in clinical orthopedics, such as, hip and knee prostheses and pins, screws, and plates since the early 1900s. When thinking improvement in material properties, such as strength and corrosion resistance, alloys have more advantageous comparing to pure metals [19]. The main considerations in selecting metals and alloys for biomedical applications are biocompatibility, appropriate mechanical properties, corrosion resistance, and reasonable cost. The physiological environment is typically modeled as 37 °C aqueous solution, at pH 7.3, with dissolved gases, electrolytes, cells, and proteins. Immersion of metals in this indicated environment can lead to corrosion which reduces the biocompatibility of materials. The electrochemical reactions leading to corrosion must be reduced or prevented. The stability of the oxides present in different metals determines their overall corrosion resistance. Ti and its alloys, stainless steel, and Co-based alloys are the three main metallic biomaterials used in load-bearing applications. When stainless steel is thought as a biomaterial; Type 316 stainless steel contains a small percentage of molybdenum (18-8sMo) to improve the corrosion resistance in chloride solution (salt water). Even, the 316L stainless steels may corrode in the body under certain circumstances in highly stressed and oxygen depleted regions, such as the contacts under the screws of the bone fracture plate, molybdenum adding results in higher strength. The other

type of metallic biomaterial, Cobalt-Chromium alloys have two types; The CoCrMo alloy [Cr (27-30%), Mo (5-7%), Ni (2.5%)] has been used for many decades in dentistry, and in making artificial joints. The CoNiCrMo alloy [Cr (19-21%), Ni (33-37%), and Mo (9-11%)] has been used for making the stems of prostheses for heavily loaded joints, as knee and hip. The two basic elements of the CoCr alloys form a solid solution of up to 65% Co. The molybdenum is added to produce finer grains, which results in higher strengths after casting. The chromium enhances corrosion resistance, as well as solid solution strengthening of the alloy. When we consider the most preferred metallic biomaterials in recent years, Titanium and its alloys are easily attract the attention because of their high strength, low weight, and outstanding corrosion resistance. More than 1000 tonnes of titanium devices of every description and function are implanted in patients worldwide every year [17]. All forms of titanium forms a thin oxide layer on the surface which have advantageous for biomedical applications[20]. The natural selection of titanium for implantation is determined by the combination of most favorable characteristics including immunity to corrosion, biocompatibility, strength, low modulus and density and the capacity for joining with bone [18]. The mechanical and physical properties of Ti alloys combine to provide implants which are highly damage-tolerant. The human anatomy naturally limits the shape and allowable volume of implants. Two further parameters define the usefulness of the implantable alloy, the notch sensitivity, the ratio of tensile strength in the notched vs. un-notched condition, and the resistance to crack propagation, or fracture toughness. Titanium scores well in both cases. Typical NS/TS (the notch sensitivity, - the ratio of tensile strength) ratios for titanium and its alloys are 1.4 - 1.7. Fracture toughness of all high strength implantable alloys is above $50\text{MPa}^{1/2}$ with critical crack lengths well above the minimum for detection by standard methods of nondestructive testing [21]. Commercial pure titanium (Cp-Ti), $\text{Ti}_6\text{Al}_4\text{V}$, and $\text{Ti}_6\text{Al}_4\text{V}$ ELI have been basically developed for structural materials although they are still widely used as representative Ti alloys for implant materials. Low modulus alloys are nowadays desired because the moduli of alloys are required to be more similar to that of bone. They are composed of nontoxic elements such as Nb, Ta, and Zr. Pure Ti and $\text{Ti}_6\text{Al}_4\text{V}$ are also the main implant materials which are the same as those for surgical implant materials.

In Table 2.1 important mechanical properties of these metallic implant materials are tabulated. The highest fatigue strength among the metallic implants is observed in $\text{Ti}_6\text{Al}_4\text{V}$. The elastic moduli of stainless steel and Co-Cr alloys are about 10 times higher than that of

natural bone (~17 GPa), which gives complications of mechanical incompatibility. Nowadays, titanium and its alloys especially Ti₆Al₄V are widely used for orthopedic applications as well as dental implants. These materials are biocompatible, highly corrosion resistant, exhibiting a modulus of elasticity of 110 GPa, 5 times greater than that of natural bone [19].

Table 2.1. Mechanical properties of metallic biomaterials [19].

Metals	Young's Modulus(GPa)	Tensile Strength(MPa)	Hardness (Vickers,kg/mm²)	Fatigue Strength(MPa)
Ti	110	300-740	120-220	240
Ti₆Al₄V Alloy	120	860-1140	310	280-660
Stainless Steel	190	500-950	130-180	260-280
Co-Cr Alloy	210	665-1277	300-400	200-300

Typical stress-strain behavior of various kinds of biomaterials used in orthopedics and natural bone are schematically illustrated in Figure 2.1 [19]. For cortical bone replacement, metals, ceramics and bioactive ceramics ensure adequate strength requirements, while others satisfy the strength requirement for the cancellous bone replacement. According to Wolff's law [22], if stiffer implant material is placed into bone, the bone will be subjected to reduced mechanical stress that gradually leads to bone resorption. The law helps us understand how to encourage bone remodelling and avoid bone stock loss. In simple terms, bone grows in response to mechanical stress. Because of that, although metals are the good choices for hard tissue implantation, they are not suitable when stress-shielding phenomenon is considered.

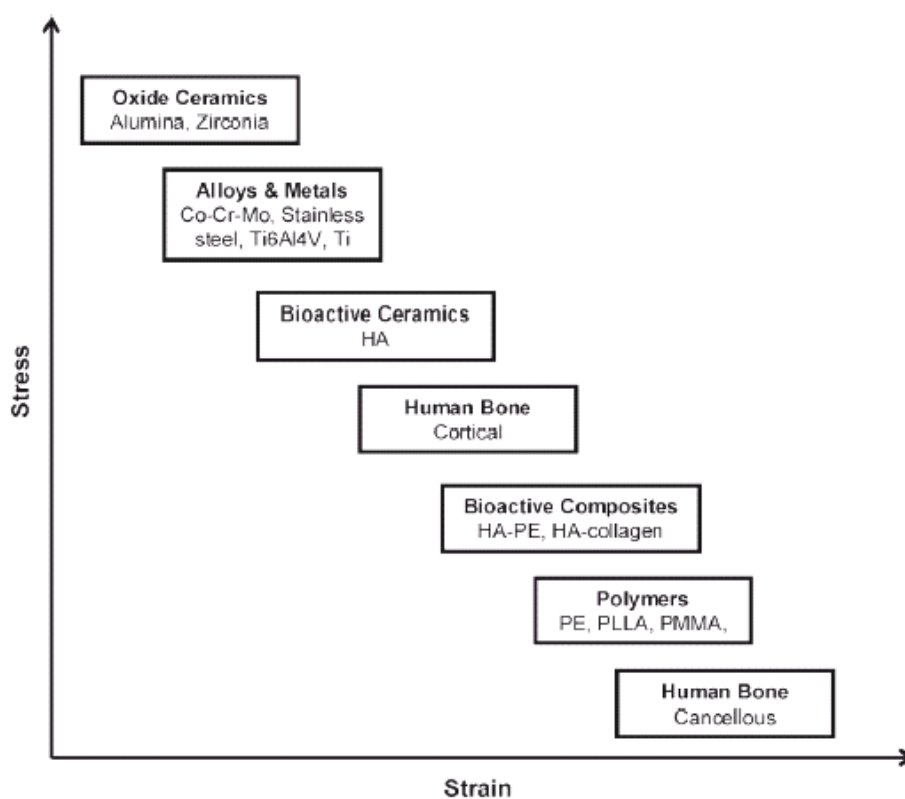


Figure 2.1. Typical stress–strain relationships of a variety of bone implants [19].

2.1.2. Ceramics

The strong ionic and covalent bonds make ceramics hard and brittle. They are also highly biocompatible and tissue responsive. The ionic and covalent nature of ceramics also influences their chemical behaviour. Although they do not undergo corrosion, ceramics are susceptible to other forms of degradation when exposed to the physiological environment. Bioceramics are used as bioinert and bioactive. Bioactive refers to materials that form bonds with living tissue. Bioactive ceramics bond directly to living bone, show osteoconduction, through a bone-like apatite layer formed on their surfaces after implantation in bony defects. However, the application of bioactive ceramics still limited because bioactive ceramics are harder and more brittle than bone. One of the most important uses of bioactive ceramics is as a filler for bioactive composites, because the mechanical properties of natural bone result from the composite structure of bone matrix [23]. Bioactive ceramics include synthetic HA, tricalcium phosphate and bioactive glass-ceramics and they are used for artificial bone. Bioinert refers to a material that retains its structure in the body after implantation and does

not induce any immunologic host reactions. The clinical use of bioinert bioceramic started in 1970 with alumina owing to its excellent biocompatibility, hardness, strength to resist fatigue, and corrosion resistance. The important mechanical properties of widely used bioceramics are listed in Table 2.2.

Table 2.2. Mechanical properties of metallic biomaterials [19].

Bioceramics	Young's modulus(GPa)	Tensile Strength (GPa)	Compressive Strength (GPa)	Hardness (HV)	Density (g/cm³)	Bond Strength (GPa)
Alumina	390	0.31	3.9	2000	3.9	300-400
Zirconia	205	0.42	3	1150	6	200-500
HA	80-110	0.05	0.4-0.9	600	3.16	120

When compare to metallic biomaterials, the bioceramics have poor tensile properties and they are brittle, lead to use them as substitute element in biomedical applications.

A common feature of bioactive materials is that their surfaces develop a biologically active hydroxy carbonate apatite (HCA) layer after implantation, which is essential for establishing bonding with natural bone [24].

2.1.3. Polymers

Polymers are the most widely used materials in biomedical applications, including orthopedic, dental, soft tissue, and cardiovascular implants due to their biocompatibility, design, accessibility, functional groups availability, surface modifiability. Polymers can be categorized into two groups which are biodegradable polymers (polyglycolic acid, polylactic acid and chitosan) and non-biodegradable polymers (polyethylene and polyethyleneterephthalate). Polyglycolic acid (PGA) is an FDA (Food and Drug Administration) approved polymer for resorbable sutures. Polylactic acid (PLA) is a similar polymer that is used for screws and plates in bone repair devices. Futhermore, combining

these PGA and PLA polymers creates the copolymer, polylactic-co-glycolide (PLGA) which is a strong resorbable implant for bone replacements with controllable properties. The crystallinity, strength and degradation are controlled by the ratio of LA to GA [21]. It is also possible to modify the end of each polymer chain in order to change the polymer properties through function groups present on polymers [21]. Polymers either natural or synthetic are long chain molecules that consist of a large number of small repeating units. Acrylic, nylon, silicone, polyurethane, ultrahigh molecular weight polyethylene and polypropylene are the commonly used polymers for orthopedic applications. The mechanical and thermal behavior of polymers are influenced by several factors, including the composition of the backbone and side groups, the structure of the chains and the molecular weight of the molecules. The mechanical properties of the typical polymers used in biomedical applications are listed in Table 2.3 [23]. They all have low elastic moduli and tensile strength, hindering their use in hard tissue replacement.

Table 2.2. Mechanical properties of typical polymeric biomaterials [21].

Material	Modulus (GPa)	Tensile Strength (MPa)
Polyethylene	0.88	35
Polyurethane	0.02	35
Polytetrafluoroethylene	0.5	27.5
Polyacetal	2.1	67
Polymethylmethacrylate	2.55	59
Polyethylene terephthalate	2.85	61
Silicone rubber	0.008	7.6
Polysulfone	2.65	75

Polyvinyl alcohol (PVA) , which presents many excellent properties such as chemical properties stability, low cost and well biocompatibility, has been widely studied as a potential artificial replacement material [25-26]. However, beside these properties their low mechanical properties let researches to use PVA as organic additives, as binder [27]. These organic additives have great effects on the microstructures and properties of ceramics. The PVA additive decreases the size of lamellar pores and increases the porosity of bioceramics [27].

2.1.4. Composite Materials

Composite materials contain two or more distinct constituent materials or phases, on a microscopic or macroscopic size scale. The properties of the composite materials depend very much on the structure as they do in homogeneous materials.

Composites differ from homogeneous materials because considerable control can be achieved over the larger scale structure to have the desired properties. In particular the properties of a composite material depend on the shape of the inhomogeneties, on the fraction of constituents, and on the interface among the constituents [23].

2.2. Calcium Phosphate Minerals

2.2.1. Calcium Phosphate Minerals

Ca-P coatings for bone-interfacing implant devices have been investigated for dental and orthopedic applications since the early 1970's [28]. The main intention for such coating was to improve the long-term biocompatibility of metallic implants by establishing a barrier coating to inhibit corrosion and associated metal ion release from metallic substrate in vivo, appropriate mechanical properties and reasonable cost. The mechanical behavior of calcium phosphate ceramics strongly influences their application as implants. Tensile and compressive strength and fatigue resistance depend on the total volume of porosity. Most calcium phosphate bioceramics can only be used as powders, or as small, unloaded implants with reinforcing metal posts, coatings on metal implants, low-bonded porous implants where bone

growth acts as a reinforcing phase and as the bioactive phase in a composite because of their low reliability under tensile load.

Calcium phosphate (CaP) biomaterials are available in various physical forms (particles or blocks; dense or porous). One of their main characteristics is their porosity. The ideal pore size for bioceramic is similar to that of spongy bone. Macroporosity is intentionally introduced into the material by adding some substances or porogens (naphthalene, sugar, hydrogen peroxide, polymer beads, fibers, etc) before sintering at high temperatures. Microporosity is formed when the volatile materials are released. Microporosity is the result of the sintering process, where the sintering temperature and time are critical parameters.

Table 2.3. Physical Properties of Calcium Phosphates [23].

Property	Value
Elastic Modulus (GPa)	40-117
Compressive Strength (MPa)	294
Bending Strength (MPa)	147
Hardness (Vickers, GPa)	3.43
Poisson's Ratio	0.27
Density (Theoretical, g/cm ³)	3.16

Table 2.5 [29] indicated some of the major calcium phosphate minerals' symbols and their Ca/P ratio. Their solubility and speed of hydrolysis increase with decreasing Ca/P ratio, for this reason only certain compounds are useful for implantation in the body. Tooth enamel has a Ca/P ratio of 1.59-1.63, and underlying dentin has a Ca/P ratio of 1.61. Bone has been

reported to have a Ca/P ratio of 1.65-1.71 .

Table 2.4. The major calcium phosphates [23].

Calcium Phosphates	Symbols	Ca/P
Monocalcium phosphate anhydrous	$\text{Ca}(\text{HPO}_4)_2$	0.50
Monocalcium phosphate monohydrate	$\text{Ca}(\text{HPO}_4)_2 \cdot \text{H}_2\text{O}$	0.50
Dicalcium phosphate anhydrous	CaHPO_4	1.00
Dicalcium phosphate dihydrate	$\text{CaHPO}_4 \cdot 2\text{H}_2\text{O}$	1.00
Octacalcium phosphate	$\text{Ca}_8\text{H}_2(\text{PO}_4)_4 \cdot 5\text{H}_2\text{O}$	1.33
Alpha tricalcium phosphate	$\text{Ca}_3(\text{PO}_4)_2$	1.50
Beta tricalcium phosphate	$\text{Ca}_3(\text{PO}_4)_2$	1.50
Hydroxyapatite (HA)	$\text{Ca}_{10}(\text{PO}_4)_6(\text{OH})_2$	1.67
Tetracalcium phosphate	$\text{Ca}_4(\text{PO}_4)_2\text{O}$	2.00

2.2.2. Hydroxyapatite

Synthetic calcium phosphate has been shown to be quite similar, crystallographically and chemically, to the natural materials in the bone[30]. Hydroxyapatite (HA) bioceramics as bone substitute materials have the advantages of abundant supply, low cost and absence of immunogenicity [30]. Apatite [$\text{Ca}_{10}(\text{PO}_4)_6\text{X}_2$] materials have unique biocompatibility feature among phosphate groups; X in the formula represents hydroxyl (OH^-) group for hydroxyapatite (HA). In particular, porous HA implants have served as bone substitute in the clinics for long time. Porosity is required for two purposes: weight reduction and the ability to rapidly deliver calcium to support histological processes. HA with controlled porosity is analogous to the natural ceramic in the bone and is bioactive in the sense that it is a non-toxic compound and interfacial bonds are able to develop between HA and the living tissues leading to enhanced mechanical strength of the overall structure. The porosity aids in tissue growth and their binding with the HA. However, lower mechanical strength of pure HA has

hampered its use as a bone implant material because of conflicting requirements of porosity and strength. So, in many uses HA mixed with additives and coated on substrates.

Pure HA has the theoretical composition of 39.68 wt.% Ca, 18.45 wt.% P, 38.22 wt.% O and 3.38 wt.% OH, with Ca/P ratio of 1.67. Hydroxyapatite forms a hexagonal rhombic crystal structure with a space a six-fold c-axis perpendicular to three equivalent a-axis (a_1 , a_2 , a_3) at angles 120° to each other [31].

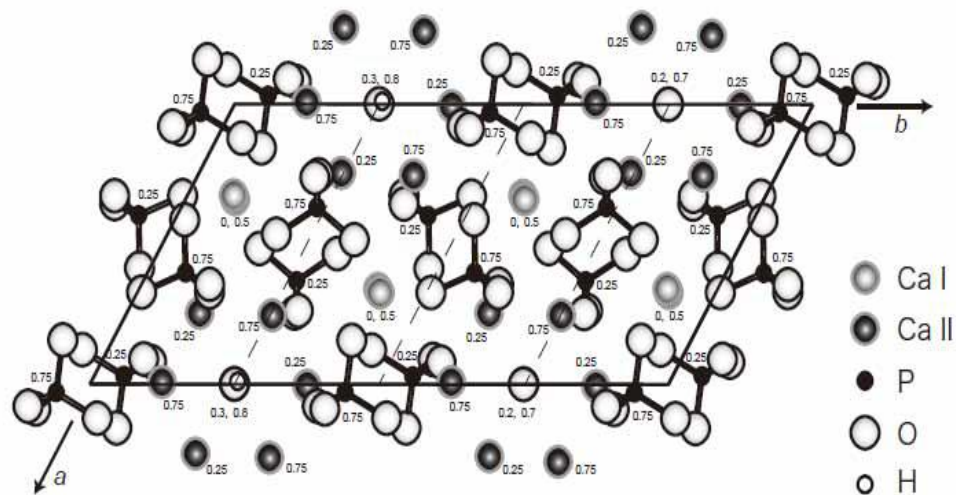


Figure 2.2. The crystal structure of HA [31].

Unit cell consists of Ca, PO_4 and OH groups closely packed together. Hydroxyl ions (OH) sit at the corners of the basal plane. These ions are positioned at every one half the unit cell, parallel to the c-axis and perpendicular to the basal plane. Thus 60 % of calcium ions in the unit cell are associated with the hydroxyl ions. The hydroxyapatite lattice contains two kinds of calcium positions columnar and hexagonal.

HA is not only bioactive but also osteoconductive and non-toxic. The bonding of bone to HA occurs by physicochemical bonding as bone cell proteins interact with HA to form direct ionic, electrostatic, hydrogen, and van der Waal bonds. The osteoconductive nature of HA coatings results in the formation of strong bonds with bone.

Table 2.5. Physicochemical, mechanical, and biological properties of HA [33].

Properties	Experimental Data
Chemical composition	$\text{Ca}_{10}(\text{PO}_4)_6(\text{OH})_2$
Ca/P molar ratio	1.67
Crystal system	Hexagonal
Young's Modulus (GPa)	80-110
Elastic Modulus (GPa)	114
Compressive Strength (MPa)	400-900
Bending Strength (MPa)	115-200
Density(g/cm ³)	3.16
Relative Density(%)	95-99.5
Hardness (HV)	600
Decomposition Temperature(°C)	> 1000
Melting Point(°C)	1614
Biocompatibility	High
Bioactivity	High
Biodegradation	Low
Cellular-compability	High

Both mechanical strength and bioactivity of HA depend strongly upon its microstructure such as grain size and grain size distribution, porosity and its shape and distribution, and material crystallinity [33]. This leaves much freedom in the hands of

materials designers to improve and tailor the properties of this material depending upon the application.

There are many techniques that have been used for hydroxyapatite coatings on metallic implant materials. Dip coating, electrophoretic deposition, hot isotatic pressing, pulsed laser deposition, sol-gel processing, thermal spraying, biomimetic process and sputter coating have been used to deposit hydroxyapatite coatings.

2.3. Hydroxyapatite Coating Techniques

2.3.1. Electrophoretic deposition

Electrophoretic deposition is a flexible, rapid, and low-cost technique depositing of metallic and non-metallic particles on electrically conductive substrates [34]. In the study of Duchnye about electrophoretic deposition technique, negatively charged colloidal HA particules suspended in a solution migrate to the substrate to be coated (an anode) by applying an electric field to the suspension [35]. The resulting film is weakly bonded to the substrate; studies employed a post deposition heat treatment at temperatures up to 900 °C to improve mechanical properties of the coating. In the later study [36], he proposed the use of electrophoretically deposited Ca-P coatings with porous titanium for understanding the effect of Ca-P films and film processing factors for bone ingrowth. The role of underlying titanium was found to be especially significant; P diffusion into the substrate accounted for a significantly higher Ca/P ratio for the coating near the interface

2.3.2. Thermal Spraying

Thermal sprayed coating methods have been used for at least 40 years. A wide range of materials can be thermal sprayed for a variety of applications, ranging from turbine technology to the biomedical industry. Different substrates can be coated using different coating materials for different applications. Zinc, aluminum, and zincaluminum alloy coatings are important anticorrosive coatings. For infrastructure applications polymer or plastic coatings have also been developed. HA coatings have been used on medical prosthetic devices and implants such as joint replacement. Thermal Spray allows to feed metallic,

ceramic, and some polymeric materials in the form of powder, wire or rod into a torch or gun where they are heated to near or somewhat above their melting point [37]. Thermal spray coatings consist of many layers of thin, overlapping, essentially lamellar particles. As the material is introduced into the spray gun, the particles receive thermal energy from the high velocity gas and melt into droplets. The droplets receive kinetic energy from the high velocity gas and move towards the target where they impinge upon the surface. On contact with the target surface, the droplets transfer thermal energy to the substrate through conduction and revert back to a solid. As they cool, they shrink, inducing a mechanical interlocking structure. Substrate surface is an important parameter to achieve coating process. For this reason, the substrate needs to be cleaned to remove any contaminants at surface. Thermal spray processes may be classified as either combustion or electric processes. Combustion processes include flame spraying, high-velocity oxyfuel (HVOF) spraying, and detonation flame spraying. Electric processes include arc spraying and plasma spraying.

2.3.3. Plasma Spray Coating

One of the most popular method in current practice for coating metal substrates with HA is the plasma spray method, one of the thermal spraying methods. Here, the HA particles are melted with plasma flame at extremely high temperatures of over 10,000 °C, and repeatedly sprayed onto the titanium plate at a speed of 100-200 m/s for layer formation. The plasma spraying method was one of the first HA film coating methods to be used, and therefore many industrial examples have been reported. However, the process of solidification requires rapid cooling from a critically high temperature, and it is not easy to control the thickness of the film layers. Generally, the HA coating formed by the plasma spray method is thick, and contain impurities such as calcium oxide in an amorphous matrix, mixed in with highly crystalline HA, resulting in an inconsistently distributed structure with uneven density and uneven adhesive properties. The stability upon implantation becomes problematic. In order to overcome the issues, treatments are continuously renovated to increase the smoothness and to improve stability. Heat treatment in solutions such as pseudo-body fluid is the main method in current practice, and the recrystallization of an HA.

Advantages of plasma spraying include a rapid deposition rate and sufficiently low cost [38]. However, there are problems associated with plasma-sprayed coatings, including

poor adhesion and variation in bond strength between the coatings and metallic substrates [39] and the extremely high processing temperature. Moreover, plasma spraying cannot provide uniform coatings on the porous metal surface or porous coatings [35].

2.3.4. Biomimetic Method

To provide the basic information allowing the suitability of a material for implanting into the human organism, the artificial materials improved for implants are tested by *in vivo* methods (in live animal organism) and by *in vitro* tests (in simulated body fluid). In the *in vitro* tests, the material is exposed to the effects of aqueous solutions simulating the inorganic part of blood plasma in the presence or absence of cell cultures, and the interactions of the surface with the solution are examined.

Kokubo *et al.* [40] proposed that the essential requirement for an artificial material to bond to a living bone is the formation of bonelike apatite on its surface when implanted in the living body. Hence, *in vivo* apatite formation can be reproduced in a SBF with ion concentrations nearly equal to those of human blood plasma [40]. Moreover, *in vivo* bone bioactivity of a material can be predicted from the apatite formation on its surface in SBF. Since then, *in vivo* bone bioactivities of various types of materials have been evaluated by apatite formation in SBF. However, the validity of this method has not been systematically assessed.

Cho *et al.* [41] reported a detailed recipe for the preparation of SBF. The recipe involved a solution which was richer in Cl⁻ ion and poorer in HCO₃⁻ ion than human blood plasma. Takadama *et al.* [42], proposed an improved SBF (n-SBF) in which only the Cl⁻ ion concentration decreased to the level of human blood plasma, leaving the HCO₃⁻ ion concentration equal to that of the corrected SBF (c-SBF). This improved SBF was compared with the corrected, conventional, c-SBF with respect to its stability and the reproducibility of apatite formation on synthetic materials. Both SBFs were subjected to round robin testing at ten research institutes. As a result, it was confirmed that the c-SBF does not differ from n-SBF in stability and reproducibility. Through this round robin testing, the method for preparing c-SBF was carefully checked and refined so that the SBF could be easily prepared. Conventional SBF with the refined recipe was proposed to the Technical Committee

ISO/TC150 of International Organization for Standardization as a solution for in vitro measurement of apatite-forming ability of implant materials in 2003.

Recently, many researchers have been interested in biomimetic preparation of coatings on the implanted material since this method has shown some advantages in comparison with the traditional methods. It can be applied to any temperature sensitive substrate because it is a low temperature process and can be deposited even on the porous substrates. Since the first formulation proposed by Kokubo *et al.*[40] for the simulated body fluid calcifying solution (SBF), concentration of individual component in the model solution were also changed and various pre-treatments were applied. Not only bulk samples but also compact samples were tested. An immersion period of the classical biomimetic CaP coating is about 14-28 days. Researchers have been focused on making this process shorter [43-45].

2.3.5. Sol-gel Method

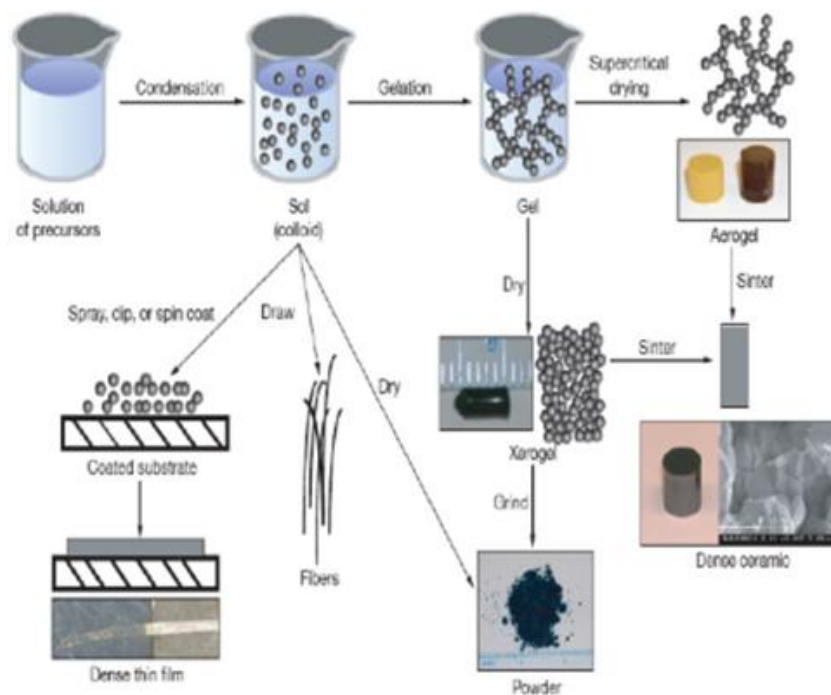


Figure 2.3. Schematic representation of sol-gel method

Sol-gel process is an industrially promising technique for preparation of thin films on large area substrates as it offers advantages in terms of low consumption of energy, low

material consumption rate, simplicity and speedy deposition on small as well as large area substrates with good homogeneity without the requirement of expensive equipment. The only drawback of this technique is that the post deposition heat treatment of the substrate at several hundred degrees Celsius is required to remove hydroxyl and organic functional groups, which limit the substrate to be a thermostable material.

Sol-gel reactions occur in a series of metal alkoxides (MA) hydrolysis and condensation reactions. As early as the mid 1800s, interest in the sol-gel processing of inorganic ceramic and glass materials has begun with Ebelman and Graham's studies on silica gels [46]. In the 1950's, Roy and co-workers synthesized a variety of novel ceramic oxides with relatively high levels of chemical homogeneity using sol-gel method.

2.3.6. Dip Coating Method

Thin films formed by a dip-coating process represent one of the oldest commercial applications of sol-gel technology. Fundamentals of sol-gel dip coating method were described by C. Jeffrey Brinker and Alan J. Hurd [13]. Dip coating is a simple process for depositing a thin film of solution onto a plate, cylinder, or irregularshaped object. The fact that the geometry of the substrates can vary widely is a distinguishing feature of the dip-coating technique [47].

The dip coating method composes of three stages. These are start-up and immersion, deposition and drainage, and evaporation.

In the dip-coating approach, there are six competing forces acting in the film deposition region that determine the position of the streamline which determines the film thickness [13]. Since the sol-gel coating with low viscosity is deposited at slow withdrawal speed, the viscous drag and gravity forces are not balanced by the applied film thickness. To properly balance the forces, a modification of the liquid-vapor surface tension, γ_{Lv} , is imposed by the liquid-vapor interface, which leads to the following film thickness relationship

$$h = 0.94(\eta U_0)^{2/3} / \gamma_{LV}^{1/6} (\rho g)^{1/2} \quad [13] \quad (2.1)$$

where h is the coating thickness, η is the solution viscosity, U_o is the withdrawal rate, ρ is the density of the sol, and g is the gravitational acceleration.

Thin film formation by sol-gel process followed by dip coating method can be used in wide variety applications when controlling chemical, physical and structural properties of thin film is crucial. Moreover, various materials can be used as coating materials onto numerous different materials. Gan *et al.* [48] obtained CaP/HA coatings from both inorganic and organic sol-gel routes onto several different materials.

In the study of Guo *et al.*[11], the HA coatings were fabricated on commercial titanium substrates with inorganic sol of $Ca(NO_3)_2 \cdot 4H_2O$ and $(NH_4)_2 \cdot HPO_4$ and organic sol of $Ca(NO_3)_2 \cdot 4H_2O$ and $PO(CH_3)_3$ by dip-coating technique to investigate the effect of firing temperature on mean crystallite size and micro strain. After firing at 400 °C, 500 °C, 600 °C, respectively, the morphology of coatings and interface properties between coatings and Ti substrate were characterized with SEM. And finally they found that, precursor type, that is, organic sol-gel and inorganic sol, greatly affected the aggregating sizes of particles for nano-HA coating, but firing temperature significantly influenced the mean crystallite size and micro-strain.

The necessity of controlling the aging time of the precursor sol as function of the sol temperature to obtain a monophasic HA coating was shown by Regi *et al* [28]. For this purpose, aqueous solutions of calcium nitrate and triethyl phosphite were chosen due to the rapid hydrolyzation of alkyl phosphates and also because the presence of oxidant agents such as nitrate anions would favor the decomposition of ethyl groups during the synthesis process. HA films deposited by dip-coating using different precursor-sols with varying ethanol/water ratios were used to coat metallic surfaces in order to establish the optimum conditions for the technological development of the sol-gel technique. Nanocrystalline carbonate hydroxyapatite coatings onto metallic substrates were prepared with different ethanol/water content. It was shown that, a control of the aging time was necessary to avoid the formation of a mixed surface coating layer. All the investigated sols formed uniform and homogeneous film on the substrate while the presence of ethanol increased the uniformity of the coating. The HA coatings obtained showed good peeling strength, 20 MPa, and a bioactive behavior under in vitro conditions, inducing bone-like apatite formation on the surface when immersed

in SBF.

In the study of Saini *et al* [49] a stable sol solution was prepared by partial hydrolysis of titanium tetrabutoxide using isopropyl alcohol as solvent. Uniform, hard and scratch proof coatings can be obtained from this sol solution by dip coating process onto large area glass and silica substrates. A 0.5 M TiO_2 sol was prepared by the partial hydrolysis and polycondensation of titanium tetra-butoxide with water using isopropyl alcohol (IPA) as a solvent and HNO_3 as a catalyst. Titanium tetrabutoxide and water have been taken in 1:1 molar ratio. The hydrolysis and polycondensation of titanium tetrabutoxide proceeds this reaction stops with the inclusion of two water molecules. This results in transparent solution with yellowish tinge. The solution was kept overnight before film deposition

Kim *et al* [6] coated Hydroxyapatite (HA) onto titanium (Ti) substrate with the insertion of a Titania (TiO_2) buffer layer using the sol–gel method. The bonding strength of the HA/ TiO_2 double layer coating on Ti was markedly improved when compared to that of the HA single coating on Ti.

Maviş and Taş [10] studied the development of recipes of appropriate solutions for the dip coating of HA on $\text{Ti}_6\text{Al}_4\text{V}$ substrates, using chemically precipitated hydroxyapatite precursor powders. They developed calcium hydroxyapatite (HA) dip-coating solution recipes to coat $\text{Ti}_6\text{Al}_4\text{V}$ substrates. The organic additives used in the solutions consisted of poly (ethylene glycol), glycerol, and/or gelatin. The HA dipcoating solution recipes did not require the drying of the green, coated strips under controlled humidity conditions. Calcination of the HA dip-coated $\text{Ti}_6\text{Al}_4\text{V}$ strips was performed in a nitrogen-gas atmosphere at a temperature of 840 °C. The HA coatings obtained were highly porous with the bonding strengths of 30 MPa.

In this thesis dip-coating method was used to coat hydroxyapatite (HA) on metal substrates to eliminate or decrease the crack occurrence and obtain uniform coatings. In dip coating process, metal substrates will be dipped in the HA sol by using designed and manufactured dip-coating device and withdrawn with the constant speed. Thickness of the forming deposit will be controlled by multiple dipping, varying the solution and changing the concentration of HA. After the deposition is completed, the as-deposited strips will dried and heated at different temperatures.

Table 2.6. Some of coating techniques and their advantages - disadvantages [34].

Technique	Advantages	Disadvantages
Dip Coating	<p>Inexpensive</p> <p>Coatings applied quickly</p> <p>Can coat complex substrates</p>	<p>Requires high sintering temperature</p> <p>Thermal expansion mismatch</p>
Electrophoretic Deposition	<p>Uniform coating thickness</p> <p>Rapid deposition rate</p> <p>Can coat complex shapes</p>	<p>Difficult to produce crack free coating</p> <p>Requires high sintering temperature</p>
Sputter Coating	<p>Uniform coating thickness on flat substrates</p>	<p>Line of sight technique</p> <p>Expensive</p> <p>Time consuming</p> <p>Cannot coat complex shapes</p>
Pulsed Laser Deposition	<p>As for sputter coating</p>	<p>As for sputter coating</p>
Hot Isostatic Pressing	<p>Produces dense coatings</p>	<p>Expensive</p> <p>Cannot coat complex shapes</p> <p>High temperature require</p>
Sol-gel	<p>Can coat complex substrates</p>	<p>Some process requires controlled temperature</p> <p>Expensive raw materials</p>

Table 2.7. Process parameters used in some studies about HA coating on metallic substrates

by dip-coating

REFERENCES	[9]	[10]	[3]-1	[3]-2	[11]	[12]	[13]
Powder	HA	HA	HA	HA	HA	HA	HA
Powder size	NA	NA	NA	NA	NA	2mm	NA
Suspension	HA-Etanol-Ti	HA-Ethanol	HA Organic	HA Inorganic	HA Ethanol	Calcium and EHA	TiO ₂ -HA and SiO ₂ -Ha
Substrate	Titanium	Ti	Titanium	Titanium	Alumina	Ti and Ti-alloys	Ti ₆ Al ₄ V
Withdrawal speed	15 cm/min	100mm/min	50mm/min	50mm/min	4cm/min	1mm/sec	38 cm/min.
Drying temperature	NA	90 °C	150 °C	150 °C	150 °C	130 °C	Room temp.
Heating temperature	500 °C	840 °C	400 °C -600 °C	400 °C -600 °C	500°C	400 °C -1400 °C	500 °C
Heating time	30 min	6 h	2 h	2 h	12or 24 h	10 min	60 min
Cooling temperature	150 °C	NA	NA	NA	NA	NA	Room temp.
Cooling time	1h	NA	NA	NA	NA	NA	NA
Aggregating particule size	250-300 nm	0.25 µm	25-40nm	100nm	NA	NA	NA
Adhesion strength	39.8±	30 Mpa	NA	NA	10.5±	NA	NA
	3.75 Mpa				1.4 MPa.		
Coated layer thickness	10 µm	25µm	2µm	5µm	2 µm	NA	400 nm
References	[9]	[10]	[11] 1	[11]-2	[15]	[50]	[51]

3. MATERIALS AND METHODS

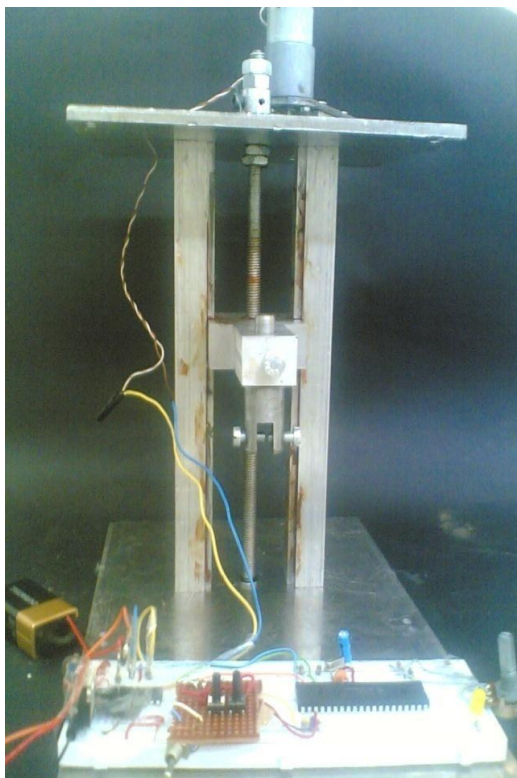


Figure 3.1. The equipment designed for dip coating method

316L Stainless Steel substrates with dimensions of 50mmx25mmx1mm thick were used. The surfaces of the substrates were abraded with 360, 600, 1000 grid SiC paper then the samples were subsequently washed with detergent in distilled water, rinsed in acetone for 20 minutes, in ethanol for 20 minutes and finally with distilled water for 30 minutes in an ultrasonic cleaner, and finally dried at 50 °C in an oven.

Dip coating solution was prepared by using the commercial HA (Calcium nitrate tribasic, $(\text{Ca}_{10}(\text{PO}_4)_6(\text{OH}))_2$ Alfa Aesar, Deutschland) by adding an organic additive, Polyvinyl alcohol (PVA). Initially, PVA was mixed with distilled water and stirred by magnetic stirrer until all the PVA powders were completely dissolved in water. The ratio of PVA to deionized water is 5 %, 7.5 % and 10 % respectively. While the stirring was continuing, the commercial powders were poured to the PVA-distilled water solution. The ratio of HA/ water was

selected as 15 %. The solution kept stirring for further 2 hours and continued with ultrasonic homogenizer for 15 minutes. HA films were obtained by dipping the metal substrates in the solution at a dipping speed of 6.6 cm/min and withdrawing them with the same speed without resting in the solution. Then the films were dried at 60 °C for 1 day and heated to 500 °C - 700 °C and 800 °C respectively, at a rate of 100 °C/h in an atmospheric oven, held there for 60 min annealing and finally cooled with the same speed to room temperature.

In the next study, the experiments were continued with the obtained films which have the optimum PVA composition for uniform, crack free coatings which was seen in 7.5 %. Therefore the study was continued with 7.5 % PVA composition at 800 °C - 900 °C and 1000 °C under vacuum to increase the corrosion resistance and increase the bonding between substrate and HA.

3.1. Materials Preparation

For the first three sets, 316L Stainless Steel plates of 50mmx25mmx7mm thick dimensions were used. Prior to coating, as the samples had been polished before, without further abraded them, they cleaned with detergent in distilled water, then washed with acetone for 20 minutes, afterwards washed with ethanol for 20 minutes and finally with distilled water for 30 minutes in an ultrasonic cleaner.

For the rest of the samples, namely 316L Stainless Steel substrates of 50mmx25mmx10mm thick dimensions were used. The surfaces of the substrates were abraded with the number of 360, 600, 1000 grid SiC paper and then washed with detergent in distilled water, continued with the same cleaning method with the first sets, and dried at 50 °C in an oven. Polishing is used to remove surface damage and haze.

3.2. Dip Coating Solution Preparation

For dip coating solution, in the first step the commercial HA powders were used. In order to determine which medium is going to be used as solvent for HA powders, distilled water and ethanol solutions with different HA-Water and HA-Ethanol concentrations were prepared. Control over the coating process is obtained if ethanol is added to the sol. The

solvent evaporation across the whole sample is uniform and control over the coating morphology is achieved. The prepared solutions were stirred by magnetic stirrer for 1 hour, and continued with ultrasonic homogenizer for 15 minutes to obtain complete dispersion. The compositions of dip coating solutions in HA films were obtained by dipping The first set of substrates in these solutions at a dipping speed of 6.6 cm/min and withdrawing them with the same speed without waiting in the HA solution. Then the films were dried at 60 °C for 2 days and heated to different temperatures between 500 °C- 1000 °C at a rate of 100 °C/h in an atmospheric oven, held there for 60 min and finally cooled with the same speed to room temperature.

In the first study, the dip coating solution was prepared according to the procedure developed by Maviş and Taş [10], shown in Figure 3.2.

Polyethylene glycol (PEG), gelatin (GEL) and glycerol (GLY) were blended with the mixture of ethanol (called EtOH) and water-HA suspension. The ingredients of the dip-coating suspensions (hereafter called SOLs) were mixed in appropriate amounts.

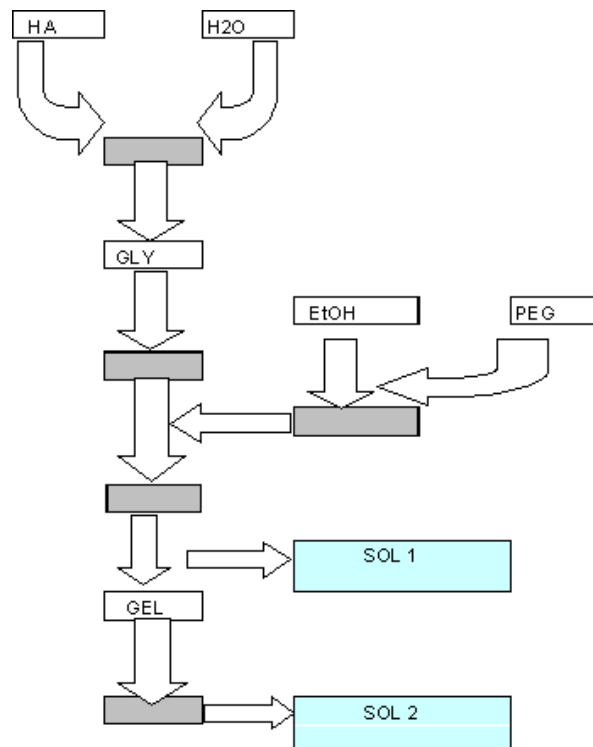


Figure 3.2. Process flowchart of the preparation of the HA dip-coating solution [10].

Then, the solution concentration is changed with the polyvinyl alcohol additive to obtain porous and crack free substrates with different sintering temperatures between 500 °C - 1000 °C.

3.3. Deposition of Sol-Gel HA Thin Films

3.3.1. Heat Treatment

3.3.1.1. Sintering. The fabrication process for ceramics normally involves several different steps. The first step in ceramics processing is compaction [52,53]. In the compaction stage, ceramic powders are pressed in a die to shape the powder into the desired form [54,55]. Heat treatment is one of the final stages of ceramics fabrication and is used to increase the strength of the compacted material [52,55].

Compacted ceramic powders undergo several significant changes during heat treatment, including but not limited to chemical reactions via decomposition and/or oxidation, phase transformations and sintering[54,55]. Sintering is a phenomenon whereby compacted powders will bond when heated to temperatures above half their melting temperature [56,57]. The goal of the sintering process is to convert highly porous compacted powder into high strength bodies [55,57]. During sintering, the significant strengthening of the ceramic body is due to the formation of inter-particle bonds resulting from atomic motion at the sintering temperature [56,57].

Sintering is driven by particle diffusion that leads to a reduction in surface energy [57]. This can occur by two possible paths, as shown in Figure 3.3. [53]. The first path is via the coarsening of the ceramic leading to an increase in the average particle size [54]. The second path is via the elimination of solid-vapor interfaces and the creation of grain boundaries, followed by grain growth that leads to densification. In the second path, the shrinkage of the compacted body has to occur. These two paths are usually competitive. If coarsening dominates, the sizes of the pores and grains of the body increase with time. If densification dominates, the pore sizes decrease and eventually disappears and the entire body shrinks [53].

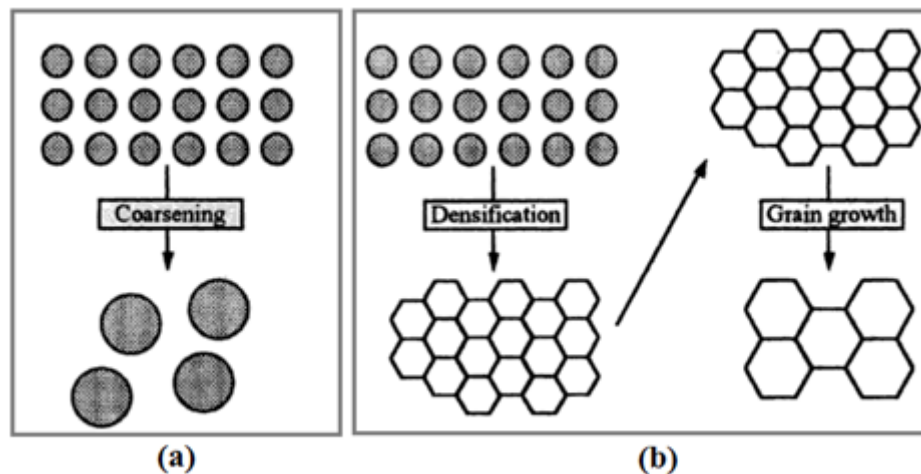


Figure 3.3. Schematic of the paths for surface energy reduction in sintering. a) coarsening where small particles combine to form larger-sized particles and 2 is b) the densification of particles followed by grain growth [53].

To understand what is occurring during sintering, the densification can be measured by dilatometry [53]. Dilatometry is a well-known method of studying densification kinetics during the sintering process of ceramic bodies [53-58]. In dilatometry, the compacted ceramic body undergoes heat treatment in the dilatometer to initiate sintering [58]. Simultaneously, the length of the compacted body is measured as a function of time at a given temperature. The densification can further be assessed by measurement of post-sintering density, whereby as the compacted body shrinks, its density will increase [53-58].

If the sintering path is via coarsening, no shrinkage will occur during the dilatometry experiment. As such, the coarsening can be examined via scanning electron microscopy to measure the average particle size [53].

There are two common types of sintering: solid-state and liquid-phase sintering [56]. Solid-state sintering is a process that converts compacted powders to strong, dense ceramic bodies upon heating [55]. Liquid-phase sintering is a process accompanied by the presence of co-existing liquid phases of liquid and solids [56]. Liquid-phase sintering is commonly used for materials which are hard to sinter and have wide applicability in industrial processes [58].

The reduction in surface energy can be used to explain the three main stages of solid-state sintering, as are shown in Figure 3.3 [55]. In the first stage, atoms migrate towards the

points of contact between particles to form necks as this filling process reduces the surface area and the surface energy [55,59,60]. In the second stage, the grain boundaries grow because, as atoms are removed from the grain boundary and diffuses towards the neck, this causes the centers of particles to mutually converge. In the final stage, the grain is slowly eliminated as grain boundaries merge [55,59,60].

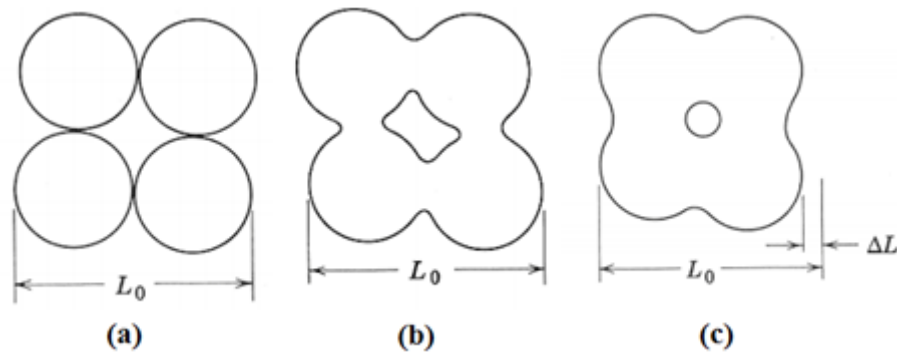


Figure 3.4. Schematic representation of the neck formation during solid-sintering due to (a) powder compaction, (b) neck growth, and (c) neck growth accompanied by densification. [53].

In liquid-phase sintering, the liquid phase can be initiated via two common techniques. In the first method, powders of different chemistries are mixed so that the interaction of the powders results in the formation of a liquid during sintering [56]. The liquid formation in this method can be a result of the melting of one component or the formation of a eutectic phase [56]. In the second method, the liquid can be formed by heating a powder to a temperature between the liquidus and solidus temperatures, resulting in co-existing liquid and solid phases [56].

Liquid-phase sintering can also be described by three phases that are driven by surface energy reduction [54,56]. In the first stage, capillary action pulls the liquid into pores so that the liquid wets the solids [53,56]. This will result in rearrangement of grains into the most favorable packing arrangement [53]. In the second stage, the liquid has a solubility for the solid and this will result in densification [56]. When smaller particles in the solids go into solution, they will preferentially precipitate on larger particles, leading to densification [56]. In the final stage, a solid skeletal network forms and the liquid moves into pores so that the wetting liquid reduces the porosity and interfacial energy of the solid phase, leading to

additional densification [56].

In the final stages of both solid- and liquid-phase sintering, the sizes of larger grains increase at the expense of smaller ones [55]. Because the sintering process is so dependent on diffusion and grain growth, particle size distributions must be carefully controlled [60,61]. A broad particle size distribution will result in hinder diffusion, abnormal boundary growth and isolation/entrapment of pores [60,61]. Studies show that powders with a narrower initial particle size distribution will result in a lower initial rate of densification before grain growth but a higher rate after [60,61].

4. RESULTS AND DISCUSSIONS

4.1. The effect of Solution Ingredients on Coating

In the study of Mavis and Tas [10] , the sintering temperature 840 °C is found to be the optimum temperature for crack free and porous coated films so in this stage all experiments are done at the same temperature with different amount of ingredients in atmospheric furnace.

Table 4.1. Different Amount of Ingredients for Solution Preparation

Samples	Sintering Temperature	Withdrawal Times	Solution	Porous/Crack Occurance
Set1	840 °C	4	8% HA+10% Ethanol	NA
Set2	840 °C	4	5% HA+20% Ethanol+10% GEL	Crack
Set3	840 °C	4	8% HA+15% Ethanol	NA
Set4	840 °C	4	8% HA+25% Ethanol	NA

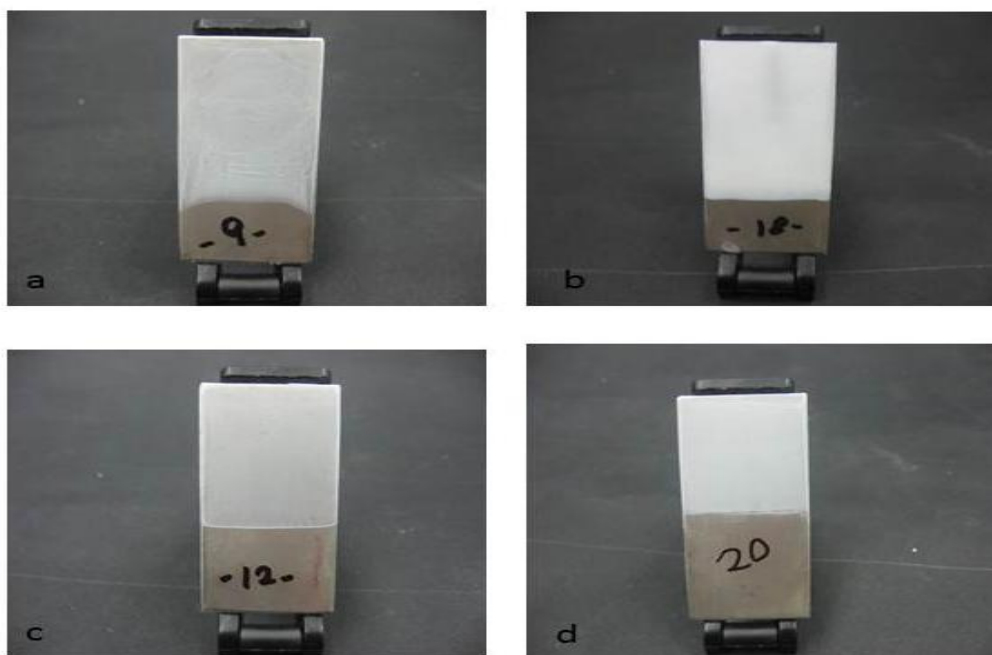


Figure 4.1. Camera images of samples(a) Set 1, (b) Set 2, (c) Set 3, (d) Set 4

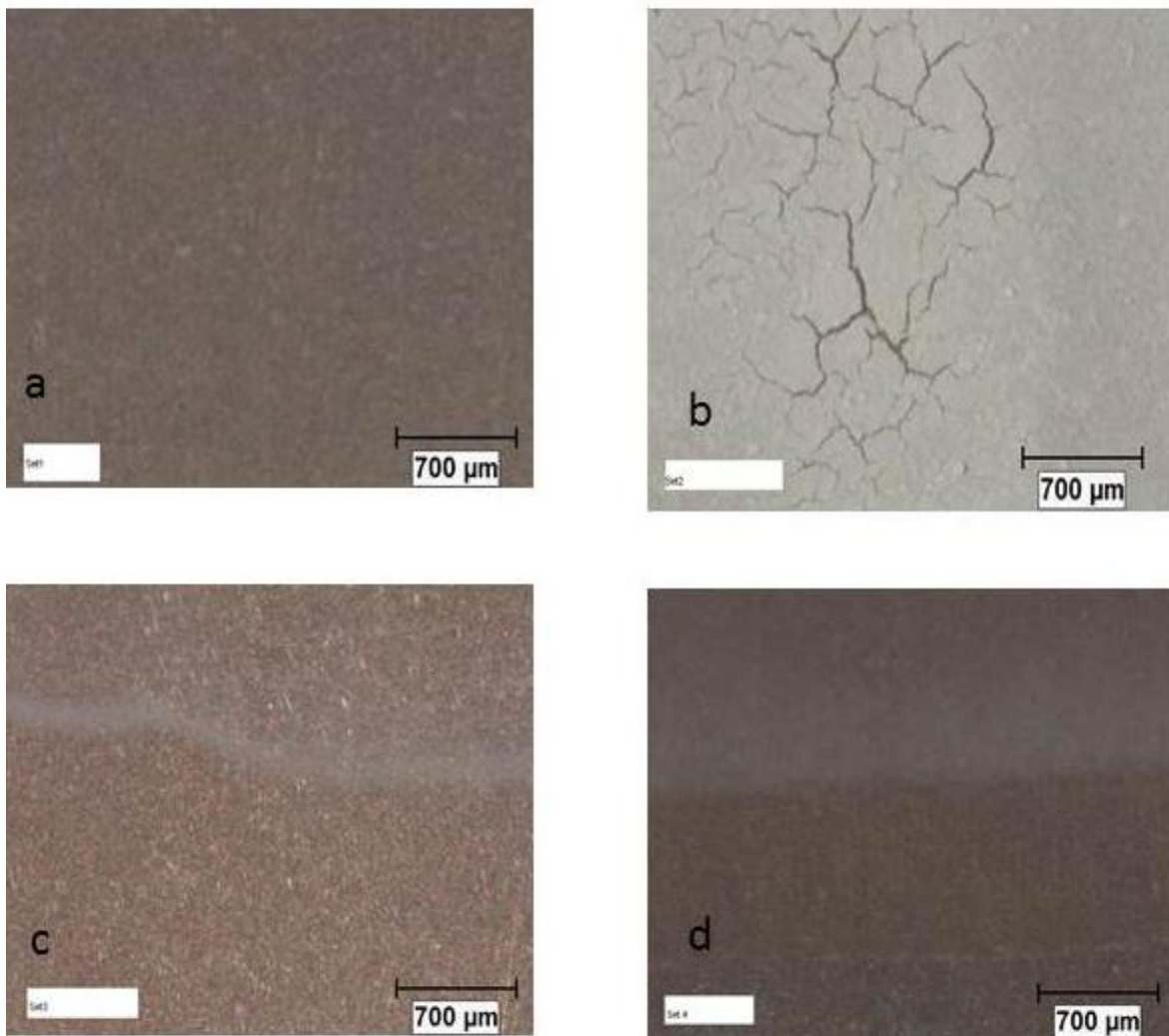


Figure 4.2: Stereo microscope images of samples (a) Set 1, (b) Set 2, (c) Set 3, (d) Set 4

The Stereo microscope images show that when the solution is prepared with adding ethanol only, HA suspension is not coated totally the metal substrates. Adding Ethanol to the solution does not have an impact on the milky like solution that coats the films. On the other hand, when adding GEL to the solution there was seen cracks were observed in the coated films. So it is thought that the crack occurrences can be because of the GEL usage or the withdrawal times.

4.2. The Effect of Withdrawal Times and GEL concentrations

The next experiments were prepared by adding GEL to all solutions with different amount and also changing the withdrawal times to find the reason for crack occurrences.

Table 4.2. Effect of Withdrawal Times and GEL concentration

Samples	Sintering Temperature	Withdrawal Times	Solution	Porous/Crack Occurance
Set5	840 °C	2	8%HA+20% Ethanol+5% GEL	NA
Set6	840 °C	2	5%HA+20% Ethanol+10% GEL	NA
Set7	840 °C	4	8%HA+20% Ethanol+5% GEL	Crack
Set8	840 °C	3	8%HA+20% Ethanol+10% GEL	Crack

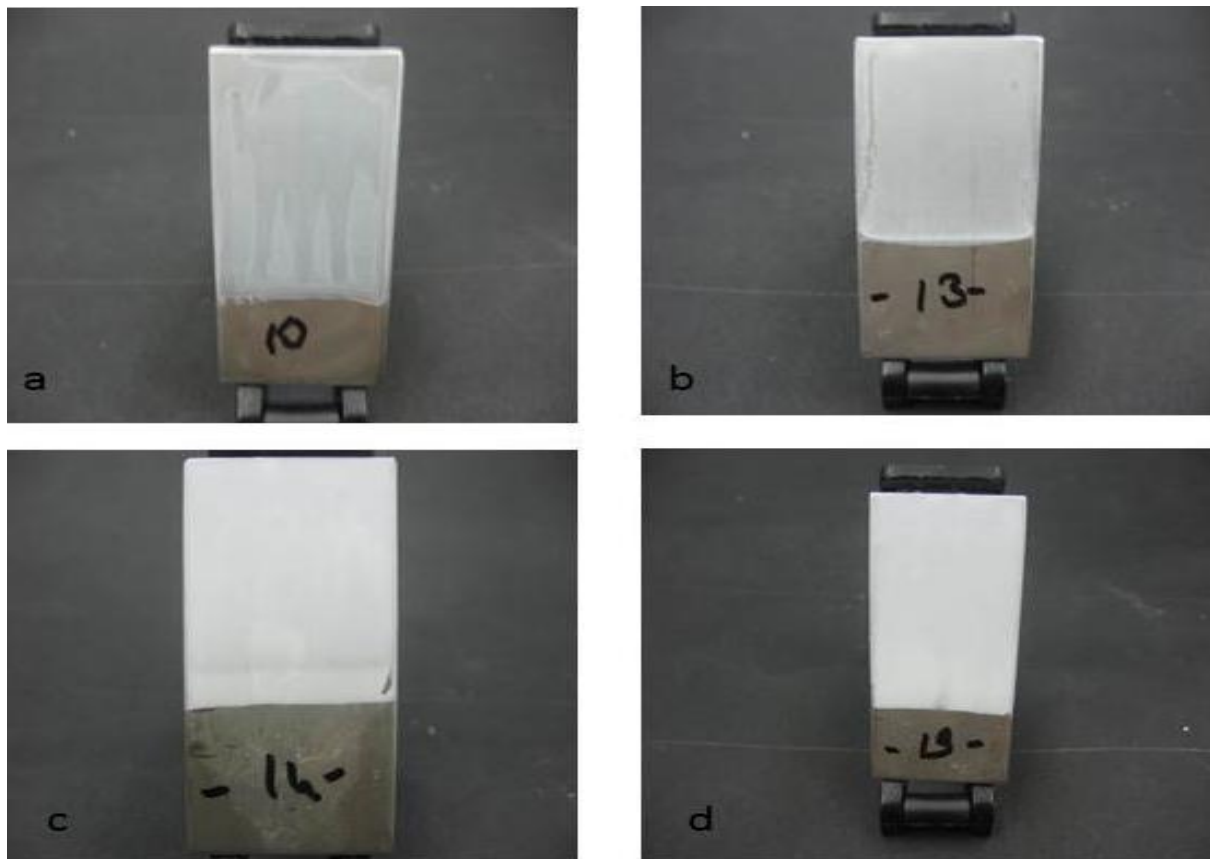


Figure 4.3. Camera images of samples(a) Set 4, (b) Set 5, (c) Set 6, (d) Set 7

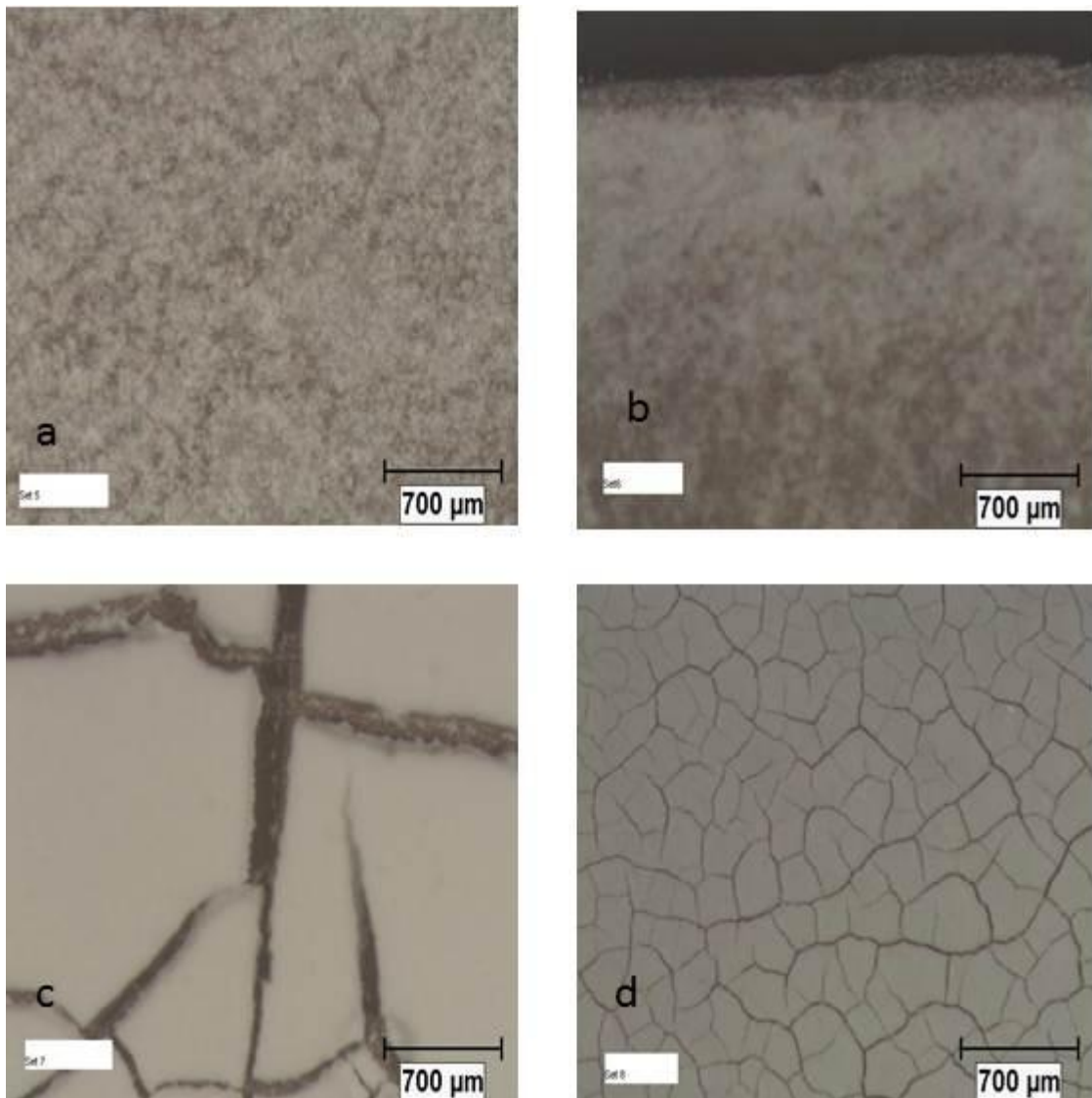


Figure 4.4. Stereo microscope images of samples (a) Set 5, (b) Set 6, (c) Set 7, (d) Set 8

According to stereo microscope images of the samples with different withdrawal times and GEL concentrations, it is seen that changing the GEL concentration of the solution does not have any significant impact on porous structure and crack occurrence, while increasing withdrawal times leads to crack occurrence due to the increasing amount of HA deposition.

4.3. The Effect of PVA additive

The next experiments were done with the additive changing from GEL to organic additive, polyvinyl alcohol (PVA) with the same sintering temperature, 840 °C with the two

different dipping/withdrawal times.

Table 4.3. Effect of different PVA additive to the solutions

Samples	Sintering Temperature	Withdrawal Times	Solution	Porous/Crack Occurance
Set 9	840 °C	2	8%HA+10%PVA	Porous
Set 10	840 °C	2	8%HA+15%PVA	Porous
Set 11	840 °C	2	8% HA+25%PVA	Crack
Set 12	840 °C	2	8% HA+40%PVA	Crack

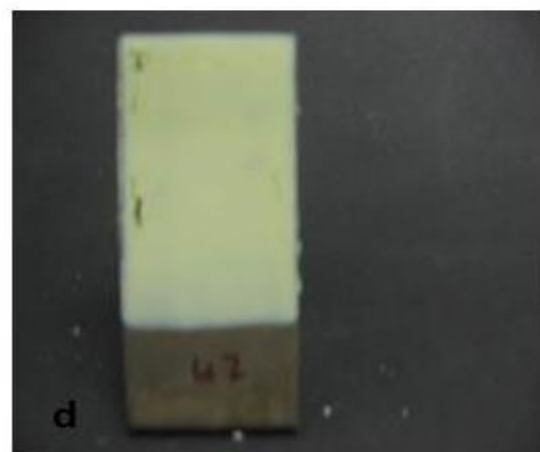
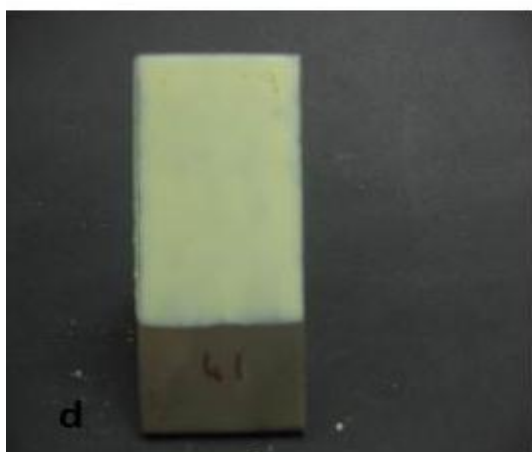
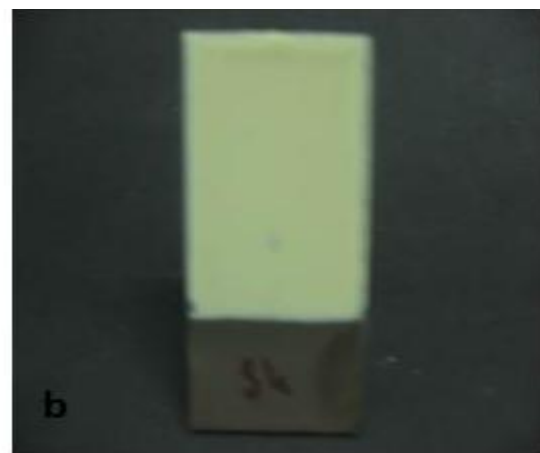
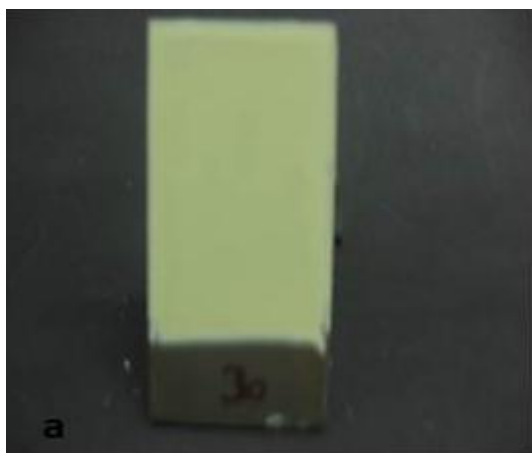


Figure 4.5. Digital camera images of samples (a) Set 9, (b) Set 10, (c) Set 11, (d) Set 12.

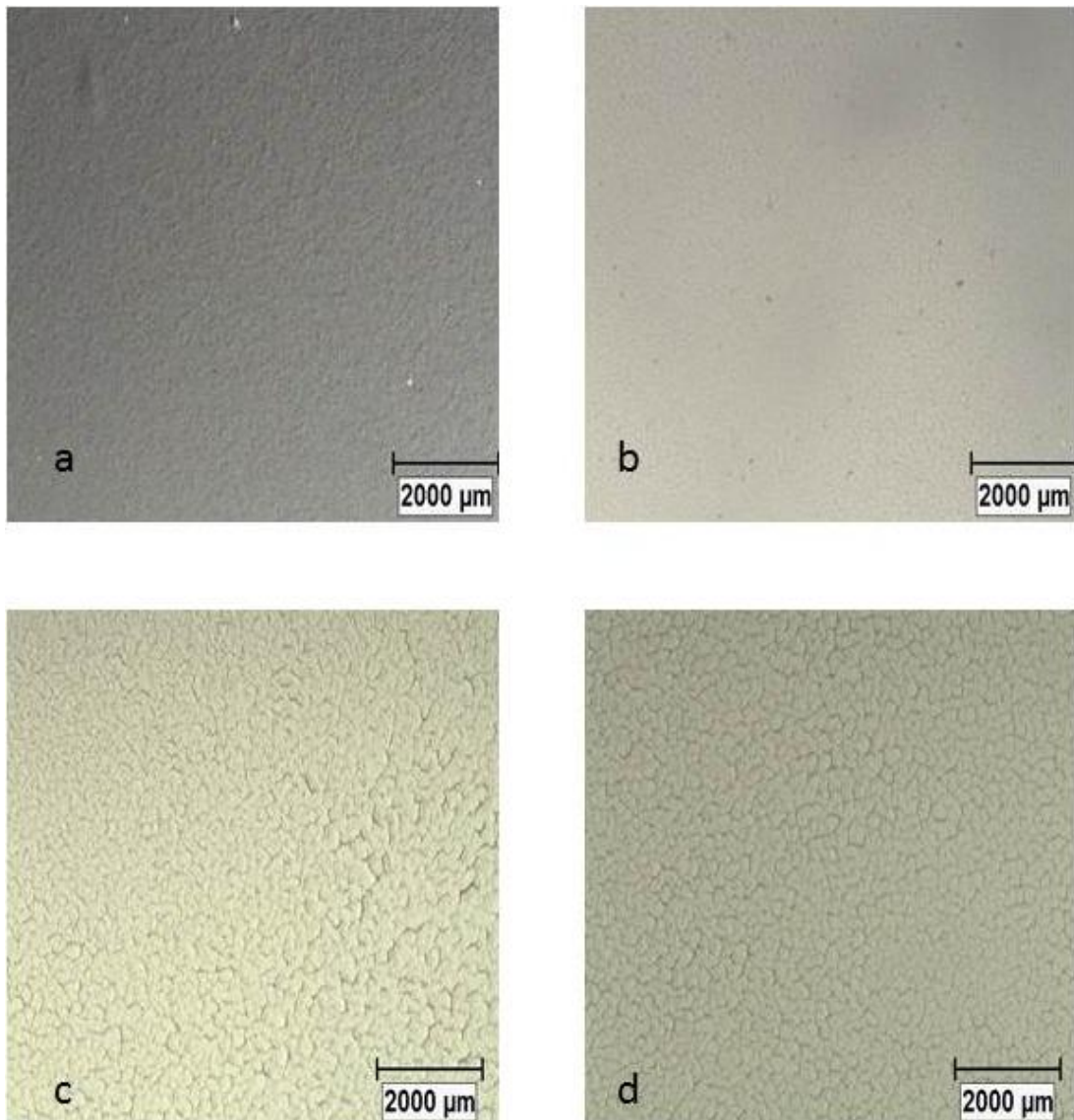


Figure 4.6. Stereo microscope images of samples (a) Set 9, (b) Set 10, (c) Set 11, (d) Set 12

According to scanning microscope images, adding PVA to the HA makes the solution milky like liquid and can make coated films which could not achieve with GEL additive. The PVA additive decreases the size of lamellar pores and increases the porosity of HA ceramics but there still crack occurrence on metal substrates when PVA concentration increases.

The next steps experiments were done in different sintering temperature with the same PVA concentrations to understand the sintering temperature effects on crack occurrences.

4.4. The Effect of Sintering Temperature

An ideal HA coated implant should be resistant to dissolution and possess high bond strength. The bond strength of the coatings is achieved by sintering. Sintered HA coatings were relatively dense and adherent to the substrate. In contrast, HA coatings for unsintered deposits can be easily removed from the substrates. Because of densification during sintering, shrinkage and cracking of the coatings can occur.

Also thermal stress induced by differences in thermal expansion coefficients between metal and the ceramic film during sintering and cooling leads to cracking. Decomposition of HA must be avoided since it results in enhanced in vitro dissolution and the formation of other calcium phosphate phases [22]. Decomposition results from dehydroxylation beyond a critical point. For temperatures below the critical point, the HA crystal structure is retained despite dehydroxylation and HA rehydrates on cooling. If the critical point is exceeded, complete and irreversible dehydroxylation occurs, resulting in the collapse of the HA structure and thus its decomposition.

Low sintering temperatures can lead to a weakly bonded low density coatings while high sintering temperatures result in degradation of the metal substrate catalysing the decomposition of HA to anhydrous calcium phosphates [14, 23]. For 316L SS it is above 1000 °C [13]. Therefore, to minimise degradation of HA and of the metal, densification temperatures ideally should be below 1000 °C. Towards this purpose, the sintering temperature was varied in the present study between 500 °C and 1000 °C for every 100 °C for a duration of 1 h each atmospheric furnace.

4.4.1. Different Sintering Temperature in Air Furnace

The surfaces of films which were heat treated in air atmosphere and vacuum furnace were both analyzed by scanning electron microscope. The first three set of them were heat treated 500 °C - 700 °C and 800 °C. in air furnace, respectively. To increase the interfacial bonding strength between the films and the metal substrates the latter three of them are heat treated under vacuum at 800 °C - 900 °C and 1000 °C, respectively.

Table 4.4. Effect of Sintering Temperature in air furnace

Samples	Sintering Temperature	Withdrawal Times	Solution	Porous/Crack Occurance
Set 13	500 °C	2	15%HA+7.5%PVA	Porous
Set 14	700 °C	2	15%HA+7.5%PVA	Porous
Set 15	800 °C	2	15%HA+7.5%PVA	Crack

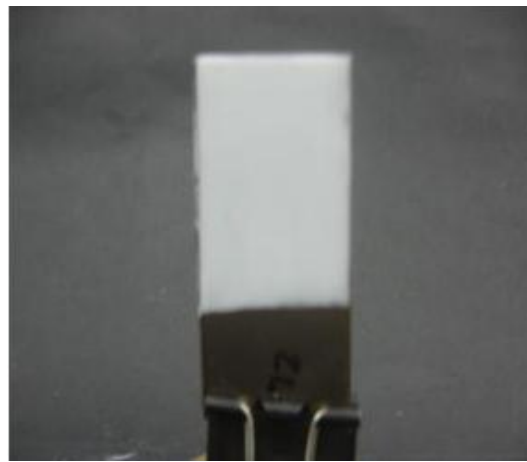


Figure 4.7. Digital camera image of the the sample in set 13

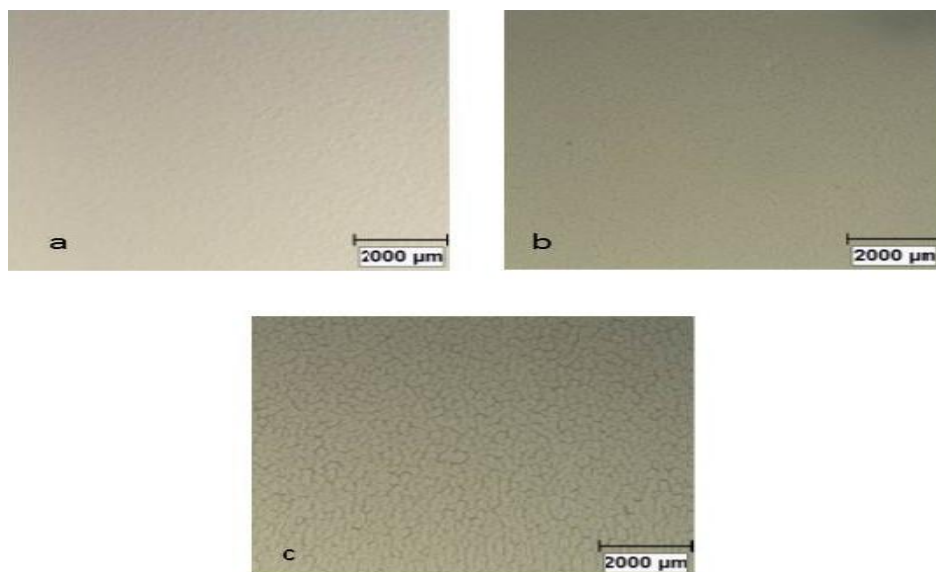


Figure 4.8. Stereo microscope image of the samples (a) set 13, (b) set 14, (c) set 15

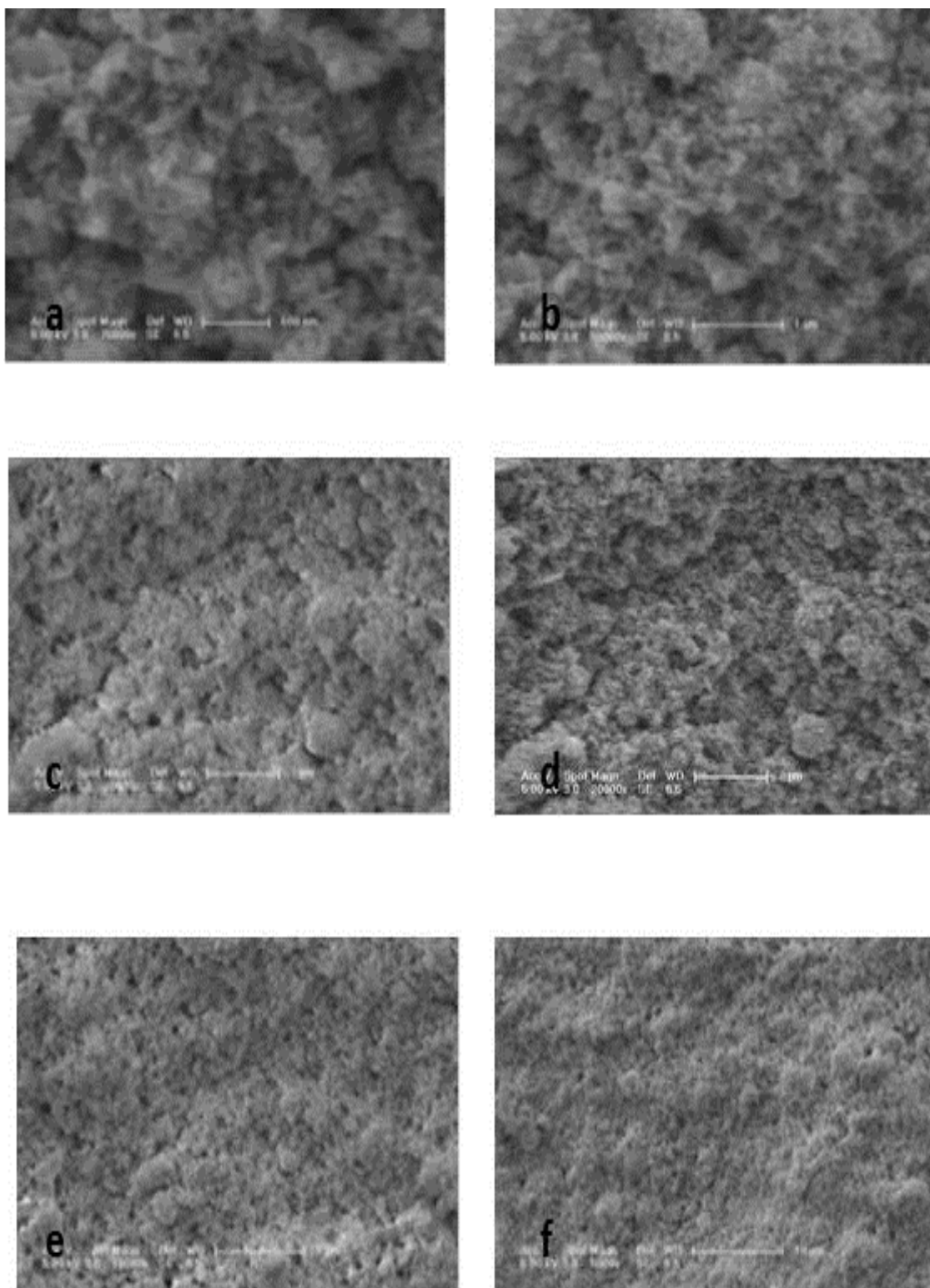


Figure 4.9. SEM images of the surface of the the sample in set 13

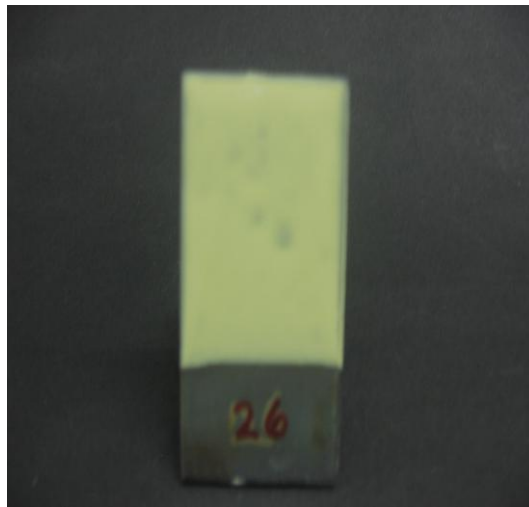


Figure 4.10. Digital camera image of the sample in set 14

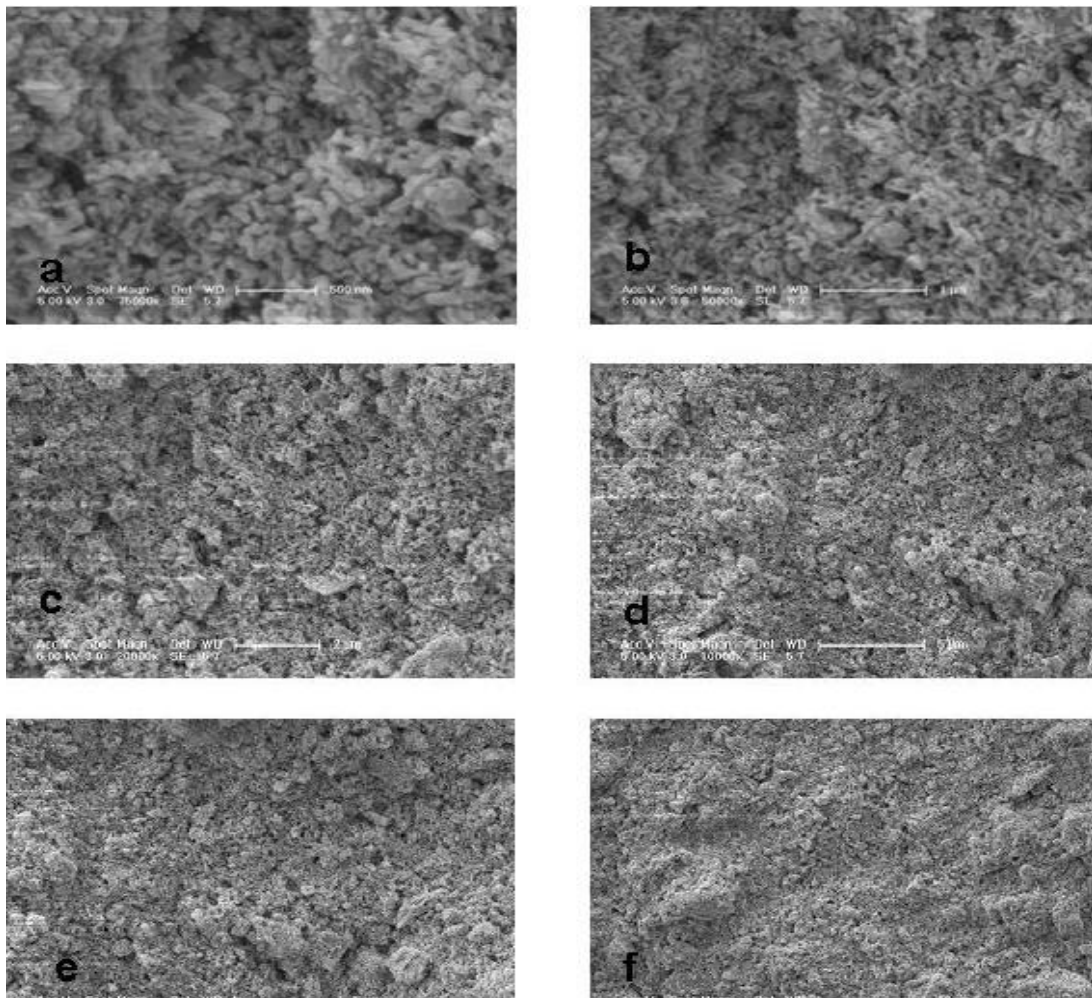


Figure 4.11. SEM images of the surface of the sample in set 14

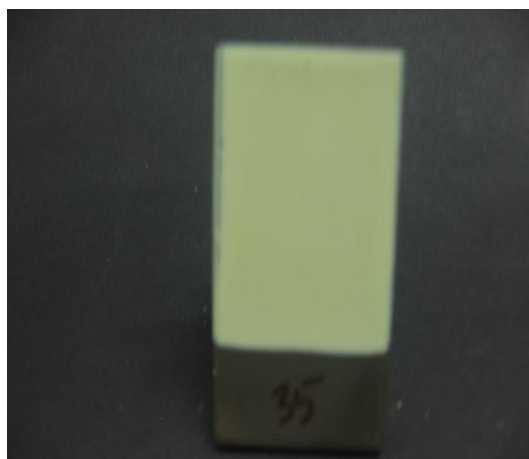
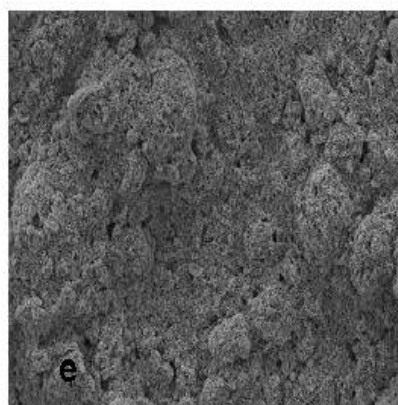
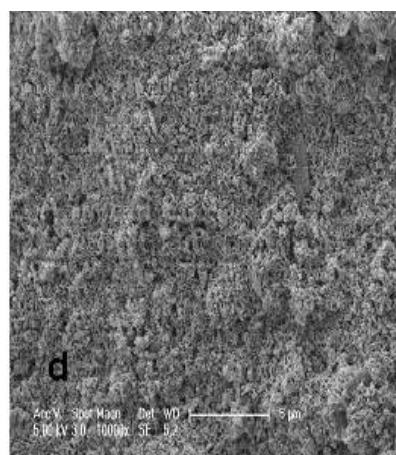
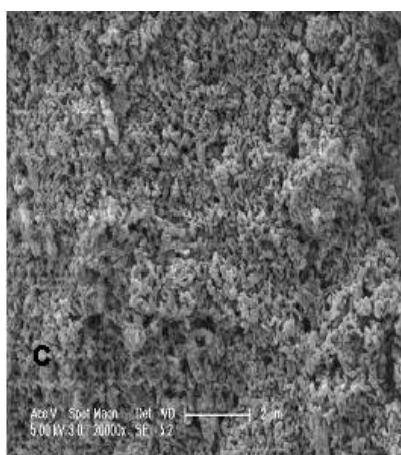


Figure 4.12. Digital camera image of the sample in set 15



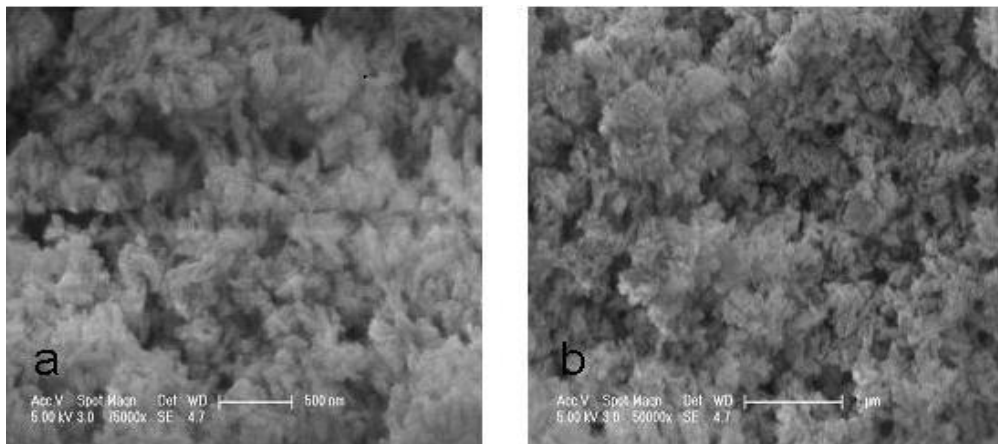


Figure 4.13. SEM images of the surface of the sample in set 15

4.4.2. The Effect of Sintering Temperature in Vacuum

Table 4.5. Effect of Sintering Temperature in vacuum

Samples	Sintering Temperature	Withdrawal Times	Solution	Porous/Crack Occurance
Set 16	800 °C	2	15%HA+7.5%PVA	Porous
Set 17	900 °C	2	15%HA+7.5%PVA	Porous
Set 18	1000 °C	2	15%HA+7.5%PVA	Crack

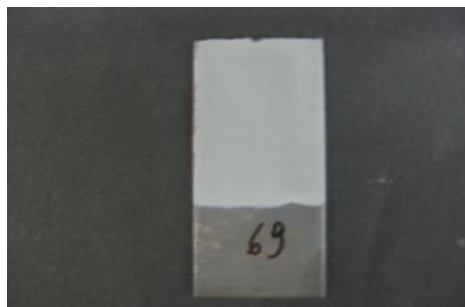


Figure 4.14. Digital camera image of the sample in set 16

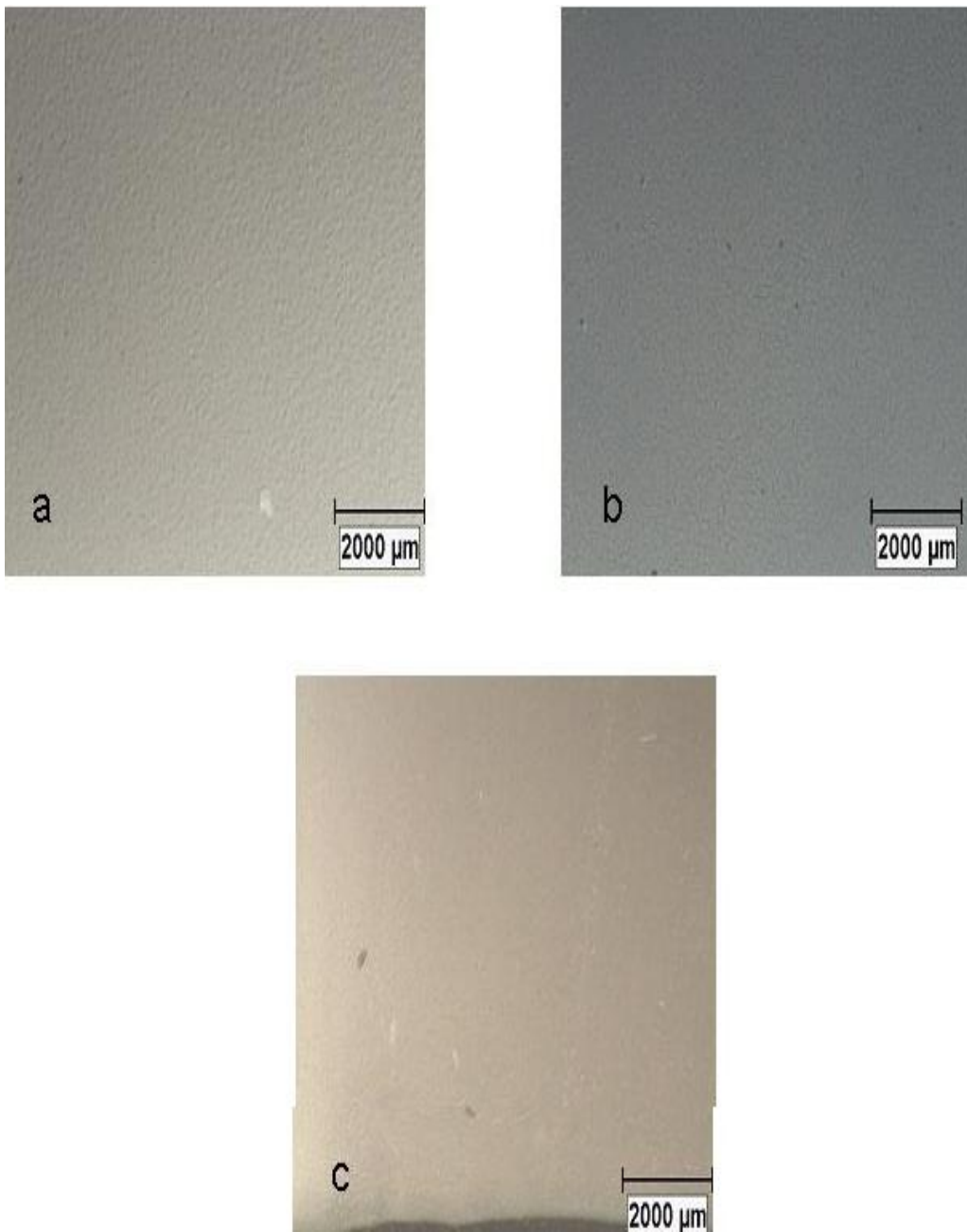


Figure 4.15. Stereo microscope image of the samples (a) set16, (b) set17, (c) set 18

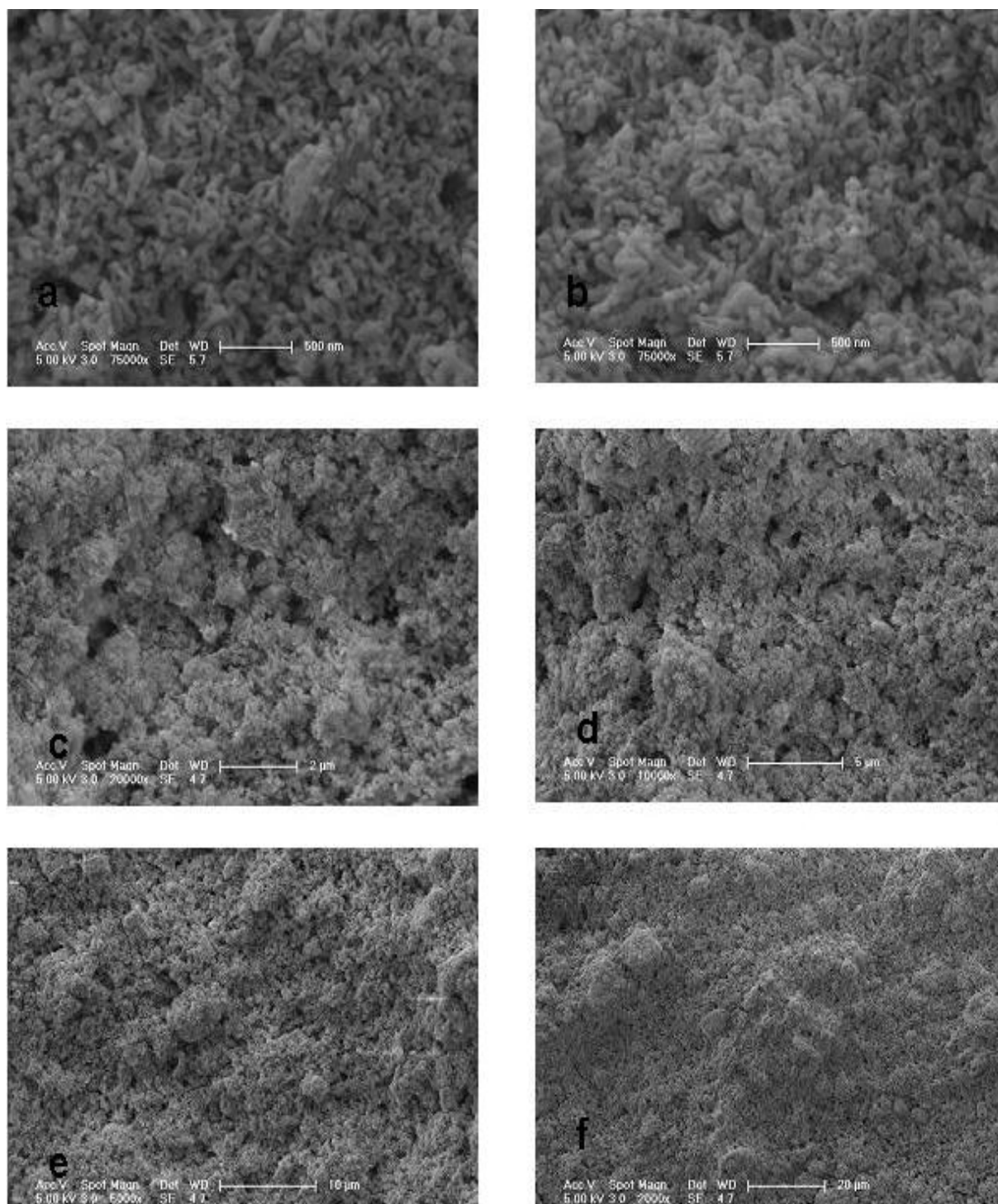


Figure 4.16. SEM images of the surface of the sample in set 16

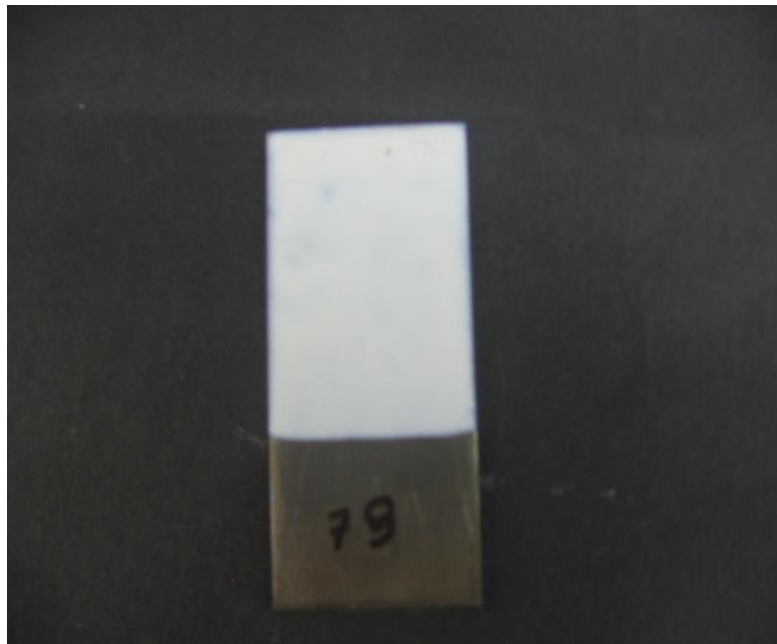


Figure 4.17. Digital camera image of the sample in set 17

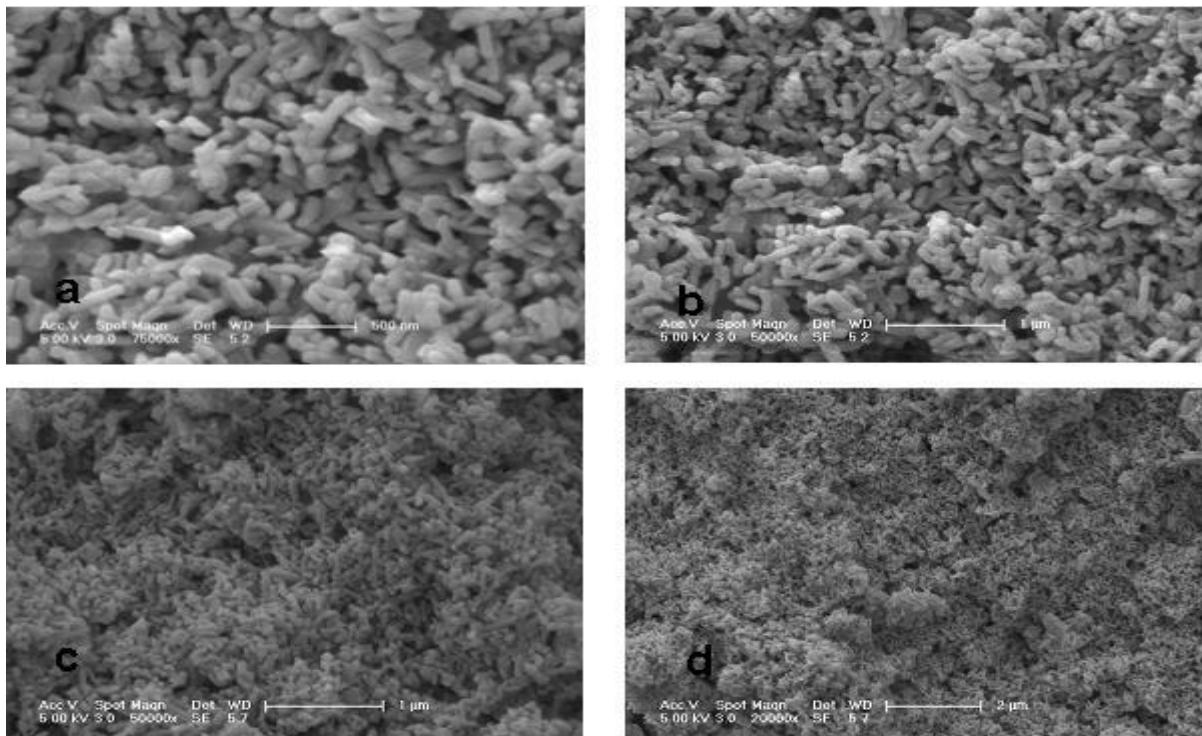


Figure 4.18. SEM images of the surface of the sample in set 17

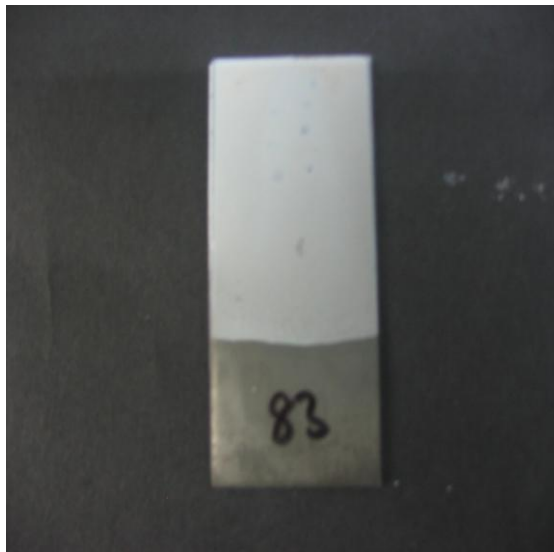


Figure 4.19. Digital camera image of the sample in set 18

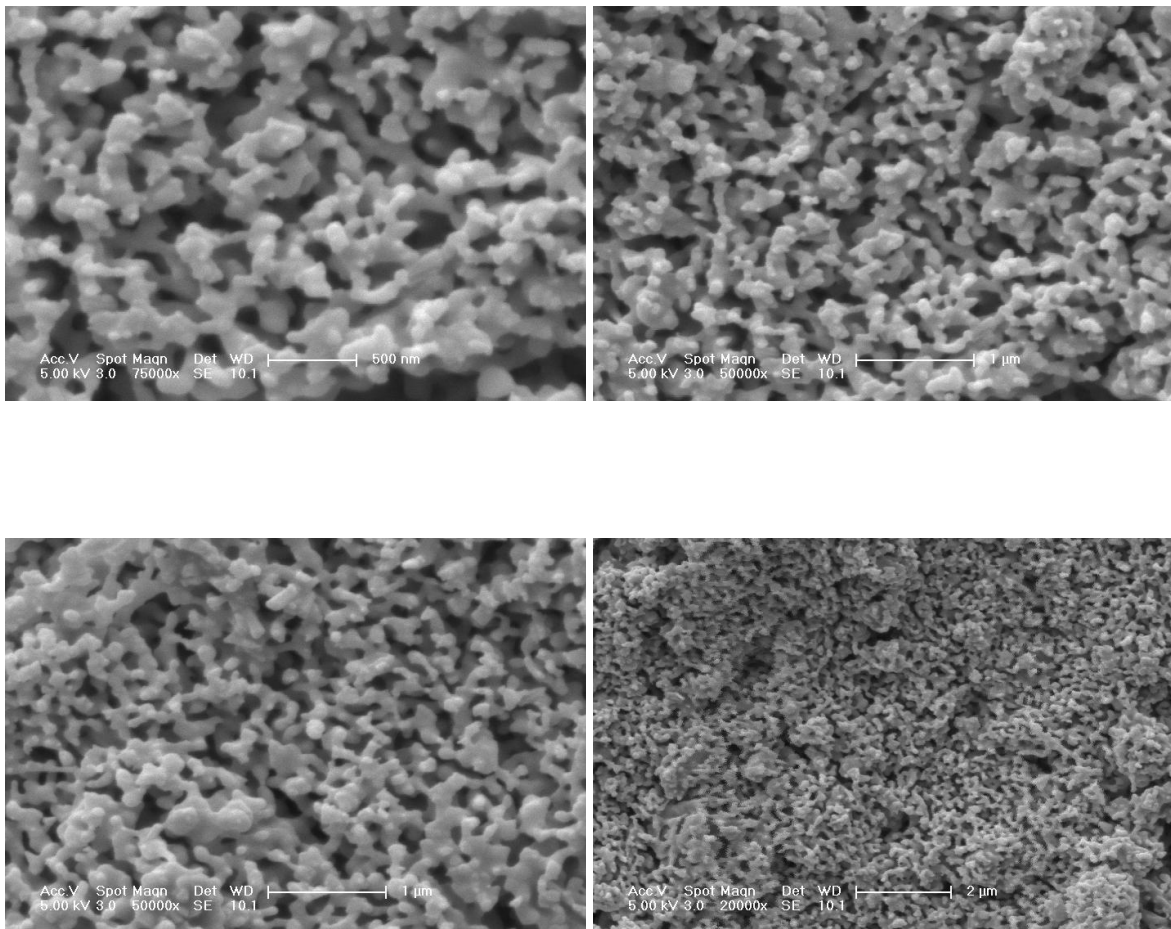


Figure 4.20. SEM images of the surface of the sample in set 18

4.5. Crack Occurance

Increasing soaking times further started to fill the originally open pores. The thicker deposit and cracks were observed at the sintering necks of the particles was believed to be due to capillary effects drawing the coating solution into this concave region as seen in the below experiment digital camera image.



Figure 4.21. Digital camera image of sample with cracks

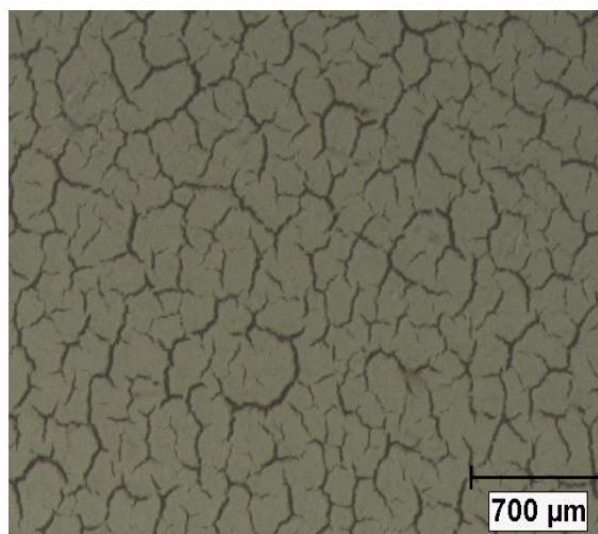


Figure 4.22. Stereo microscope images of a sample with cracks

4.6. EDAX Results



Figure 4.23. EDAX results of the sample in set 17



Figure 4.24. EDAX results of the sample in set 18

5. CONCLUSIONS

Solutions were prepared by mixing ethanol, gelatin and organic additive, PVA with HA to coat 316L stainless steel. The dip coating process was performed by using a special apparatus whose speed was kept constant at 6.6 cm/min during dipping and withdrawal. The drying of the HA dip-coated 316L Stainless Steel substrates were performed at 60 °C in air atmosphere furnace and the sintering stages were performed at temperature 840 °C for the first experiments, and then continued with 500 °C - 700 °C and 800 °C in ambient furnace and 800 °C - 900 °C and 1000 °C under vacuum. It was observed that; as the sintering temperature increased the crack occurrences increased. However using vacuum furnace instead of atmosphere furnace decreased the crack formation, and also prevent from the oxidized metal surface which will lead metal ions diffuse into the coated films causing biological system defects in the future. The remarks of the conclusion are below;

- Adding only ethanol to the solution does not effect on milky solution that coats the films.
- Increasing GEL addition to the solution does not have significant impact on crack occurrences.
- Increasing withdrawal times increase film thickness whereas crack occurrences could be seen.
- Low sintering temperature leads to weakly bonded coatings where unsintered deposits can easily be removed.
- Sintering temperature above 1000 °C leads to mismatch of thermal expansion coefficient between metal substrate and hydroxyapatite coating.
- The composition of HA suspension, withdrawal times and sintering temperature affected the morphologies of the coatings.

REFERENCES

1. Branemark, P.I., "Osseointegration and its experimental background", *Journal of Prosthetic Dentistry*, Vol. 50, pp. 399-410, 1983.
2. Sivakumar, M., U. Kamachi Mudali, S. Rajeswari, *Steel Research*, Vol. 65, pp. 76, 1994.
3. Rondeli, G., B. Vicentini, A. Cigada, *Journal of Corrosion*, Vol. 32, pp.193, 1997.
4. Yang, C.Y., B.C. Wang, W.J. Chang, *Journal of Materials Science: Materials in Medicine*, Vol. 7, pp. 167, 1997.
5. Wei, M., A. J. Ruys, M. V. Swain, S. H. Kim, B. K. Milthorpe and C. C. Sorrell, "Interfacial Bond Strength of Electrophoretically Deposited Hydroxyapatite Coatings on Metals", *Journal of Materials Science: Materials in Medicine*, Vol. 10, pp. 401-409, 1999.
6. Kim, H., Y. Koh, L. Li , S. Lee, "Hydroxyapatite Coating on Titanium Substrate with Titania Buffer Layer Processed by Solgel Method", *Biomaterials intro* Vol. 25, pp. 2533-2538, 2004.
7. Sun, L., K. A. Gross and A. Kucuk, "Material Fundamentals and Clinical Performance of Plasma-Sprayed Hydroxyapatite Coatings: A Review", *Journal of Biomedical Materials Research*, Vol. 58, pp. 570-592, 2001.
8. Albayrak, O., C. Oncel, M. Tefek and S. Altintas, "Effects of Calcination on Electrophoretic Deposition of Naturally Derived and Chemically Synthesized Hydroxyapatite", *Reviews on Advanced Materials Science*, Vol. 15, pp. 10-15, 2007.
9. Milella, E., F. Cosentino, A. Licciulli, C. Massaro, "Preparation and Characterization of Titania/Hydroxyapatite Composite Coatings Obtained by Sol-gel

Process", *Biomaterials*, Vol. 22, pp. 1425-1431, 2001.

10. Mavis, B., A. C. Tas, "Dip coating of Calcium Hydroxyapatite on Ti6Al4V Substrates", *Journal of Ceramic Society.*, Vol.83, pp. 989-991, 2000.

11. Liu, D., Q. Yang, T. Troczynski, "Sol-gel Hydroxyapatite Coatings on Stainless Steel Substrates", *Biomaterials*, Vol. 23, pp. 691-698, 2002

12. Saini, K.K., Sunil Dutta Sharma, Chanderkant, Meenakshi Kar, Davinder Singh, C.P. Sharma, "Structural and Optical Properties of TiO₂ Thin Films Derived by Sol gel Dip Coating Process", *Journal of Non-Crystalline Solids*, Vol. 353, pp. 2469-2473, 2007.

13. Brinker, C.J., Hurd A.J., "Fundamentals of Sol-gel Dip Coating" *Journal of Physics France*, Vol. 4 ; pp. 1231-1242, 1994.

14. Ebelmen, M., Ann., *Chimie Journal of Physics*, Vol. 16, pp.129, 1846.

15. Weng, W., "Sol-gel Derived Porous Hydroxyapatite Coatings", *Materials in Medicine*, Vol. 9, pp. 159-163, 1998.

16. Sridhar, T.M., S. Rajeswari, M. Subbaiyan, U. Kamachi Mudali, "Sintering Effects on Hydroxyapatite Coated Type 316L Stainless Steel and Its Impedance Behaviour in Ringers Solution, in: E.S. Dwarakadasa, C.G. Krishnadas Nair (Eds.) ", *Proceedings of the Third International Conference on Advances in Composites*, pp. 265, 2000.

17. Ratner, B. D., "Biomaterials Science :an Introduction to Materials in Medicine", *Elsevier Academic Pres*, pp.8-158, 2004.

18. David, H., "Metals in medical applications", *KohnCurrent Opinion in Solid State and Materials Science*, Vol.3, pp. 309-316, 1998.

19. Murugan, R., S.Ramakrishna, "Review:Development of Nanocomposites for Bone Grafting", *Composites Science and Technology*, Vol.65, pp. 2385–2406, 2005.
20. Lee, H.U., Y.S. Jeong, S.Y. Park, S.Y. Jeong, H.G. Kim, C.R. Cho, "Surface Properties and Cell Response of Fluoridated Hydroxyapatite/TiO₂ coated on Ti Substrate", *Current Applied Physics*, Vol 9, pp.528-533, 2009.
21. Jones, F.H., "Teeth and bones: Applications of Surface Science to Dental Materials and Related Biomaterials", *The Eastman Dental Institute for Oral Health Care Science*, 2001.
22. Harold, M., B.A. Frost, "Update of Bone Physiology and Wolff's Law for Clinicians", *Angle Orthodontist*, Vol 74, pp. 3–15, 2004.
23. Karageorgiou, V., D.Kaplan, "Review: Porosity of 3D Biomaterial Scaffolds and Osteogenesis", *Biomaterials*, Vol.26, pp. 5474-5491, 2005.
24. Deram, V., C. Minichiello, R.N. Vannier, A. Le Maguer, L. Pawlowski, D. Murano, "Microstructural Characterizations of Plasma Sprayed Hydroxyapatite Coatings.", *Surface Coat Technology*, Vol.166, pp. 153-159, 2003.
25. Hai, T., Q. Syed, "Poly(vinyl alcohol) hydrogels-2. Effects of Processing Parameters on Structure and Properties", *Polymer* 36, pp. 2531–2539, 1995.
26. Pan, Y.S., D.S. Xiong, R.Y. Ma, "A Study on the Friction Properties of Polyvinyl alcohol Hydrogel as Articular Cartilage Against Titanium Alloy ", *Wear* 262, pp. 1021–1025, 2007.
27. Zuo, K.H., Y.P. Zeng, D. Jiang, "Effect of Polyvinyl Alcohol Additive on the Pore Structure and Morphology of the Freeze-cast Hydroxyapatite Ceramics", *Materials Science and Engineering C* 30, pp. 283–287, 2010.

28. Hulbert, S.F., J.F. Bokros, L.L. Hench, J. Wilson, G. Heimke, "Ceramics in Clinical Applications", *past, present and future, in High Technology Ceramics, (Ed. P.Vincenzini)*, pp. 3-27, 1987.
29. İpekoğlu, M., "Effects of Calcination and Particulate Size on The Sintering of Natural Hydroxyapatite", M.S. Thesis, Boğaziçi University, 2005.
30. Driessens, F.C.M., "Probable Phasecomposition of the Mineral in Bone", *Zeitschrift fur Naturforschung C-A, J. Biosci. Vol. 35 (5-6)*, pp.357-362, 1980.
31. Ratner, B.D., A.S. Hoffman, F.J. Schoen, J.E. Lemons, *Biomaterials Science, Academic Press, San Diego, CA, 1996.*
32. Elliott, J.C., "Structure and Chemistry of The Apatites and Other Calcium Orthophosphates", *Studies in inorganic chemistry*, pp.18; 1994.
33. Suchanek, W., M. Yoshimura, "Processing and Properties of Hydroxyapatite-Based Biomaterials for use as Hard Tissue Replacement Implants", *Journal of Material*, Vol. 13, pp.751-762, 2002.
34. Albayrak, Ö., "Hydroxyapatite Coating on Ti and Ti6Al4V Substrates by Using Electrophoretic Deposition Method", Ph. D. Thesis, Boğaziçi University, 2008.
35. Duchheyne, P., W. Van Raemdonck, J.C. Heughebaert, M. Heughebaert, "Structural Analysis of Hydroxyapatite Coatings on Titanium", *Biometaterials*,7, pp. 97-103, 1986.
36. Duchheyne, P., S. Radin, M. Heughebaert, J.C. Heughebaert, "Calcium Phosphate Ceramic Coatings on Porous Titanium, Vacuum Sintering and in vitro Dissolution", *Biometaterials*,11, pp. 244-254, 1990.

37. Garrett, R., A. Pandit, D.P. Apatsidis, "Review:Fabrication Methods of Porous Metals for Use in Orthopaedic Applications" *Biomaterials*, Vol. 27, pp. 2651– 2670, 2006.
38. Suchanek, W., M.Yoshimura, "Processing and Properties of Hydroxyapatite-based Biomaterials for use as Hard Tissue Replacement Implants" *Journal of Material*, Vol. 13, pp. 751-762, 2002.
39. Schreurs, B.W., R.Huiskes, P.Buma , T.J.J.H. Slooff, "Biomechanical and Histological Evaluation of a Hydroxyapatite-coated Titanium Femoral Stem Fixed with an Intramedullary Morsellized Bone Grafting Technique: an animal experiment on goats", *Biomaterials*, Vol.17, pp.1177-1186, 1996.
40. Kokubo T., "Design of Bioactive Bone Substitutes Based on Biomineralization Process", *Materials Science and Engineering*, Vol. 25, pp. 97– 104, 2005.
41. Lu, X., Y. Leng, "Theoretical Analysis of Calcium Phosphate Precipitation in Simulated Body Fluid", *Biomaterials*, Vol. 26, pp. 1097–1108, 2005.
42. Kokubo, T., H. Takadama, "Leading Opinion: How useful is SBF in predicting In vivo Bone Bioactivity ", *Biomaterials*, Vol.27, pp. 2907–2915, 2006.
43. Bharati, S., M. K. Sinha., D. Basu, "Hydroxyapatite Coating by Biomimetic Method on Titanium Alloy using Concentrated SBF", *Material. Science*, Vol. 28, pp. 617–621, 2005.
44. Habibovic, P., J. Lia , C. M. Valk, G. Meijerc, P.Layrolled , C.A. Blitterswijk , K. Groot "Biological Performance of Uncoated and Octacalcium Phosphate-coated Ti₆Al₄V", *Biomaterials*, Vol.26, pp.23–36, 2005.
45. Barrerea, F., C. A. Blitterswijk, K. Groota, P. Layrolle "Influence of Ionic Strength and Carbonate on the Ca-P coating Formation from SBFX5 Solution",

Biomaterials, Vol.23, pp. 1921–1930, 2002.

46. Kim, H., Y. Koh , L. Li , S. Lee "Hydroxyapatite Coating on Titanium Substrate with Titania Buffer Layer Processed by Sol–gel Method", *Biomaterials intro*, Vol.25, pp. 2533–2538, 2004.

47. Yimsiri, P., M. R. Mackley "Spin and Dip Coating of Light-Emitting Polymer Solutions: Matching Experiment with Modeling", *Chemical Engineering Science*, Vol. 61, pp. 3496–3505, 2006.

48. Gan, L., R. Pilliar "Calcium Phosphate Sol–gel-Derived Thin Films on Porous Surfaced Implants for Enhanced Osteoconductivity. Part I: Synthesis and Characterization", *Biomaterials*, Vol.25, pp. 5303–5312, 2004.

49. Saini, K.K., S. D. Sharma, Chanderkant, M. Kar, D. Singh and C.P. Sharma "Structural and Optical Properties of TiO₂ Thin Films Derived by Sol–gel Dip Coating Process", *Journal of Non-Crystalline Solids*, Vol. 353, pp. 2469-2473, 2007.

50. Metikos, M., Hukovic, E. Tkalcec, A. Kwokal, J. Piljac, "An in Vitro Study of Ti and Ti-alloys Coated with Sol–gel derived Hydroxyapatite Coatings", *Surface and Coatings Technology*, Vol. 165, pp.40-50, 2003.

51. Zhang W., C.Wang, W. Liu, "Characterization and Tribological Investigation of Sol–gel Ceramic Films on Ti₆Al₄V ", *Wear*, Vol.260, pp.379–386, 2006.

52. Rahaman, M.N., *Ceramic Processing and Sintering*, 2nd edition, Vol.23, pp 23.,2005.

53. Barsoum, M., *Fundamentals of Ceramics*. New York: McGraw-Hill, pp.304 ,1997.

54. Reed, J.S., *Principles of Ceramic Processing*, 2nd edition New York: Wiley-Interscience, 1995.

55. Fahrenholtz, W. G., "Sintering", University of Missouri-Rolla Rolla, Labrotary Report Example , 2004.
56. German, R. M., *Liquid Phase Sintering*, Facsimile ed. New York: Plenum Press, 1985.
57. Braginsky, M., "Numerical Simulation of solid State Sintering", *International Journal of Solid Structures*, Vol. 42, p. 621 – 636, 2004.
58. Holkova, Z., "Kinetic study of Al₂O₃ Sintering by Dilatometry", *Ceramics*, vol. 47, pp. 13, 2003.
59. Kingery, W.D., *Introduction to Ceramics*, 2nd ed. New York: John Wiley and Sons, 1976.
60. Boch, P., *Ceramic Materials: Processes, Properties and Applications*, Wiltshire: ISTE, pp. 55–85, 2007.
61. Ting, J.M., R. Y. Lin, "Effect of Particle Size Distribution on Sintering", *Journal of Materials Science*, Vol. 30, pp. 2382-2389, 1995.